Journal of Geophysical Research: Earth Surface

RESEARCH ARTICLE
10.1029/2017JF004405

The Dynamics of Channel Slope, Width, and Sediment in Actively Eroding Bedrock River Systems

Brian J. Yanites[1]

[1]Department of Earth and Atmospheric Sciences, Indiana University, Bloomington, IN, USA

Key Points:
- A new approach to modeling river evolution in steep landscapes that includes channel width adjustment and sediment dynamics is presented
- Incorporating channel width adjustment and sediment transport lowers river profile sensitivity to changes in rock uplift
- Patterns of channel width and slope in transient river channels can provide insight into the underlying controls on river erosion

Correspondence to:
B. J. Yanites,
byanites@indiana.edu

Citation:
Yanites, B. J. (2018). The dynamics of channel slope, width, and sediment in actively eroding bedrock river systems. *Journal of Geophysical Research: Earth Surface*, *123*, 1504–1527. https://doi.org/10.1029/2017JF004405

Received 21 JUN 2017
Accepted 12 MAY 2018
Accepted article online 24 MAY 2018
Published online 4 JUL 2018

©2018. American Geophysical Union. All Rights Reserved.

Abstract The evolution of rivers in eroding landscapes plays a key role in determining landscape relief and modulating climate-tectonic interactions. A common approach to quantifying river system evolution uses a one-dimensional, detachment-limited stream power equation. One potential drawback of this model is that it does not incorporate the effects of changes in channel width or the role of sediment transport dynamics. Here I present a new method for modeling the influence of channel width on river dynamics to explore how variable width and sediment transport impact river profile evolution. With this approach, vertical river erosion can operate based on any number of river erosion models, such as a simple shear stress model (e.g., detachment limited), sediment cover-shear stress hybrid models, or mechanistic saltation-abrasion models. I explore the sensitivity of these three models to increases in rock-uplift rate (i.e., 2, 3, 5, 10, and 20× increase). Generally, the results show that incorporating channel width adjustment or sediment transport dynamics lowers the sensitivity of a river profile to rock-uplift rate. For the sediment transport-dependent models, the degree of sensitivity depends on whether the system is limited by bedrock exposure or erosion potential (i.e., detachment potential). The approach produces transient responses that reveal distinct patterns of width and slope, which may provide valuable insight into the limiting physical mechanisms of bedrock erosion in a region. The implications of the work are broad and include the potential to distinguish underlying erosion controls from field observations of width and slope as well as understanding climate-tectonic interactions.

1. Introduction

Bedrock rivers are a central focus in many geomorphic studies as they influence the topographic response to climate and tectonics (Roe & Brandon, 2011; Whipple & Meade, 2006; Willett, 1999), are used to map tectonics and active deformation (Chen & Willett, 2016; Duvall et al., 2004; Goren et al., 2014; Kirby & Whipple, 2001, 2012; Seeber & Gornitz, 1983; Wobus, Whipple, et al., 2006), and are integral in understanding landscape signatures of climate (Ferrier et al., 2013; Gasparini & Whipple, 2014; Murphy et al., 2016; Wobus et al., 2010). Rivers that erode bedrock exist across a range of climatic and tectonic environments (Figure 1); therefore, quantifying the response of river systems to climate and tectonics is necessary to understand how Earth systems interact in the various environments around the world.

The most common quantitative approaches to understanding and modeling river systems use a 1-D detachment-limited model of river erosion and longitudinal profile development often referred to as the stream power model (DiBiase & Whipple, 2011; Howard, 1994; Jeffery et al., 2013; Pelletier, 2007; Perron & Royden, 2013; Roberts & White, 2010; Roe et al., 2002; Whipple & Tucker, 1999). The simplicity of the model has allowed predictions of the geometric response of rivers to tectonic, lithologic, and climatic changes based on numerical and analytical forms of the equation (Forte et al., 2016; Perne et al., 2017; Roe & Brandon, 2011; Royden & Perron, 2013; Whipple, 2001; Wobus et al., 2010). The straightforward predictions and computational efficiency have led to widespread application of this model and all of its assumptions to many landscapes around the world (Lague, 2014) and to other planets in the solar system (Barnhart et al., 2009). Yet when the model assumptions are tested with independent field evidence, disparate conclusions are reached. In some cases, researchers have interpreted that the model captures the dynamics of mountainous rivers reasonably well (Crosby & Whipple, 2006; Cyr et al., 2010; DiBiase et al., 2010; Duvall et al., 2004; Ouimet et al., 2009; Snyder et al., 2000), yet in other studies, researchers found that the model fails to predict morphological changes associated with a significant variation in forcing (Cowie et al., 2008; Lague, 2014; Lavé & Avouac, 2001; Ward & Galewsky, 2014; Whittaker et al., 2007a; Yanites et al., 2010). Developing new quantitative approaches that can bridge the gaps in the observational tests of theory is needed to improve constraints on how topography evolves in a dynamic Earth system.

Figure 1. Rivers erode bedrock across a range of tectonic and climatic regimes. Examples included here are arid Utah and Arizona, semiarid Colorado and Idaho, temperate Indiana, and subtropical Taiwan. Locations also span tectonic regimes from active (Taiwan) to continental interiors (Indiana).

Two factors that may be important in bedrock river dynamics but are not represented in the stream power model are the roles of channel width and sediment dynamics in bedrock erosion (Figures 1 and 2). Observations of channel width across spatial gradients in erosion rates/rock uplift or along a river undergoing a transient response to a change in base level show a clear tendency of significant cross-channel geometry adjustments (Allen et al., 2013; Amos & Burbank, 2007; Bufe et al., 2016; Finnegan et al., 2005; Kirby & Ouimet, 2011; Lavé & Avouac, 2001; Whittaker et al., 2007a; Yanites et al., 2010). Arguments explaining these observations have been broad ranging from feedbacks associated with sediment transport and river incision (Lague, 2010; Turowski et al., 2009; Yanites & Tucker, 2010) to simple conservation of mass of fluid flow in a steepening river with a constant width-to-depth ratio (Finnegan et al., 2005). Whatever the underlying mechanism, cross-channel geometry adjustments change the erosive potential of a river, potentially absorbing part of the topographic impact that would otherwise be accommodated by channel slope if rivers behaved in a 1-D manner as prescribed by many modern river erosion models. Further, sediment has been shown to be a dominant control on river erosion processes in a number of environments including both the effects of cover in protecting bedrock (Johnson et al., 2009; Sklar & Dietrich, 2006; Yanites et al., 2011) and as tools to abrade or loosen bedrock for detachment (Brocard et al., 2016; Crosby et al., 2007; Jansen et al., 2011). Observation and modeling studies have shown that ignoring sediment processes where they are an important control on river processes leads to an overestimate of the magnitude of the topographic response to changes in rock uplift (Cowie et al., 2008; Gasparini et al., 2007).

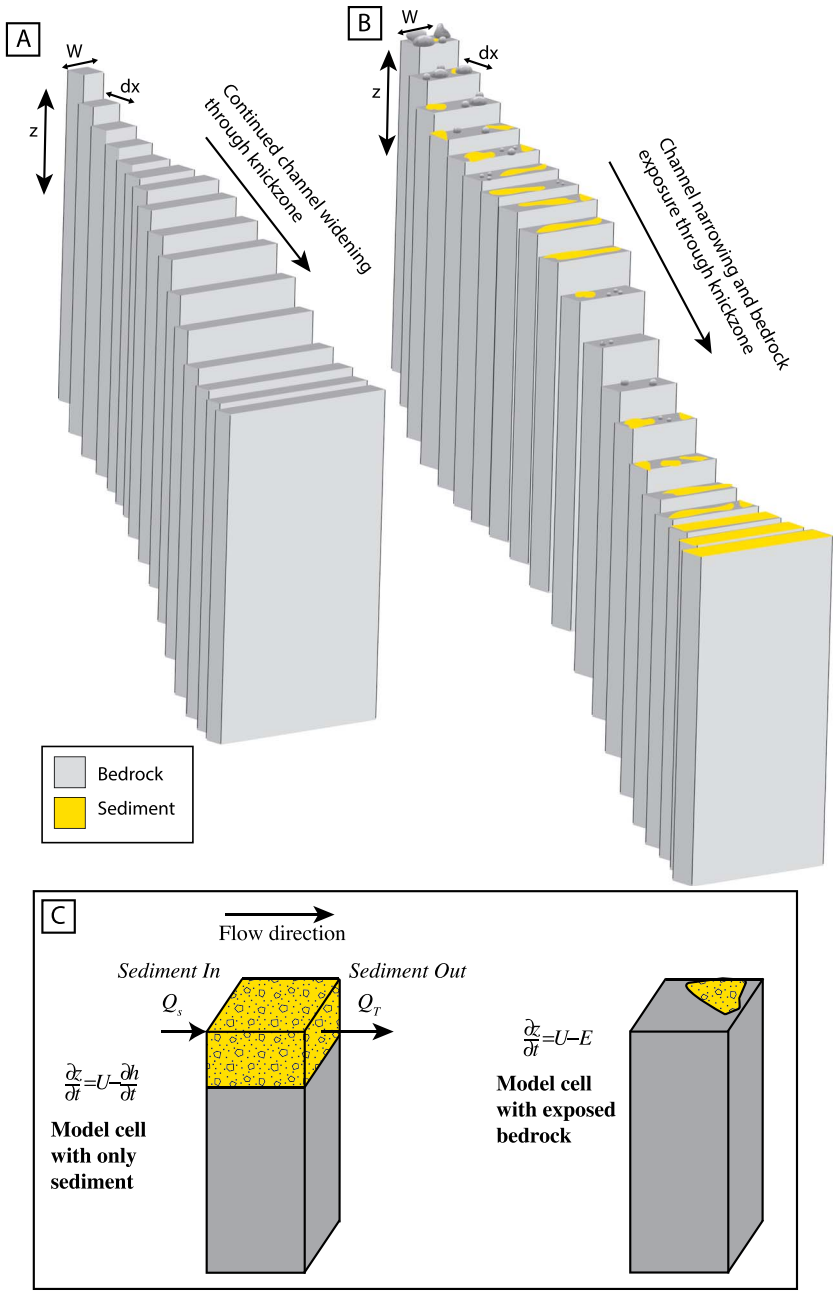

Figure 2. Schematic model setup. (a) Typical 1-D stream power river profile model for which channel width (W) varies with drainage area only. (b) Schematic of model represented by the methods proposed here. Both channel width and sediment cover evolve in response to transient perturbations such as increases in the rate of rock-uplift (U). (c) The change in elevation (z) with time depends on local rock-uplift and either the (left) conservation of sediment thickness, h, or the (right) erosion of bedrock, E. In both cases, sediment fluxes (Q_s and Q_t) are calculated to predict if the model cell is completely covered by sediment or if bedrock is exposed, except for the detachment-limited model where no sediment is modeled. See text for further explanation.

This previous work showing the importance of channel geometry and sediment transport prompts the critical assessment of slope-only river erosion models in many environments (Lague, 2014; Zhang et al., 2017) and motivates the development of a river erosion model that quantifies adjustments in both slope and width in response to changes in base level, water discharge, erodibility, and sediment supply (e.g., Hancock et al., 2011; Lague, 2010; Nelson & Seminara, 2011; Stark, 2006). Further, to understand the dynamics on landscape evolution time scales, this approach must occur in a framework that allows modeling river erosion processes over orogenic time scales. Previous work modeling the dynamic evolution of channel width has provided important insights into how channel geometry responds to tectonic or climate changes. For example, a

number of models predict the cross-sectional evolution of a bedrock channel based on simple erosion rules (Lague, 2010; Nelson & Seminara, 2011; Stark, 2006; Wobus, Tucker, & Anderson, 2006). While these models are insightful for understanding the dynamics of width and cross-channel shape, they impart several limitations to their use over long time scales or large regions: (1) Some of these approaches are computationally limiting (Wobus, Tucker, & Anderson, 2006), especially when they account for how and where sediment is transported in the channel cross section (Lague, 2010), and (2) some of the approaches introduce a number of new variables in the model that must be assumed or parameterized (Lague, 2010; Nelson & Seminara, 2011; Stark, 2006).

Here I develop a new approach to modeling river profiles that overcomes many of these limitations by leveraging an assumption of river channel optimality, which has been used to explain slope and width variations across a range of river systems (Nanson & Huang, 2008; Turowski et al., 2007, 2009; Yanites & Tucker, 2010). The approach presented here provides a computationally efficient method that only introduces one new variable, a channel width adjustment efficiency factor (k_w). I use this modeling framework to address three fundamental questions:

- How does the inclusion of dynamic width and sediment transport processes influence the sensitivity of the evolution of bedrock river profiles to tectonic change?
- What is the transient response of river width and slope to changes in tectonic rock uplift?
- Can observations of channel width along channels provide insight into the physical mechanisms controlling erosion in bedrock rivers?

Addressing these three questions will advance understanding of river dynamics in landscapes actively eroding underlying bedrock and improve the ability to quantify the interaction of climate and tectonics.

2. Model

The modeling framework includes rock uplift, which acts to lift the river bed relative to a stable reference frame, and river processes, which include both the sediment transported as bedload and fluvial bedrock erosion (Figure 2). At each time step, vertical channel evolution (bedrock incision rate and/or change in sediment thickness) and width changes are quantified as described below. The presented model is not a replacement to these more physically based approaches, but rather provides a complementary approach that is useful for incorporating channel width dynamics over long time scales and large spatial scales. Additionally, one of the goals of the model development here is to provide a framework for incorporating dynamic channel width and the impacts of sediment into landscape evolution models.

Elevation (z) along the river profile evolves over time (t) and is modified by the rock-uplift rate (U_r) and either the erosion rate (E) or the change in the sediment thickness (h) if the entire bed of a reach is covered in sediment:

$$\frac{\partial z}{\partial t} = \begin{cases} U_r - E & \text{if h} = 0 \\ U_r + \dfrac{\partial h}{\partial t} & \text{if h} > 0 \end{cases} \tag{1}$$

The implementation of this model is schematically illustrated in Figure 2 and is similar to other river profile modeling approaches (Yanites et al., 2013). Over long time scales (e.g., $>10^3$ yrs), sediment depth (h) will be greater than zero if sediment supply outpaces capacity. In this case, vertical erosion will cease until this sediment is evacuated. If sediment transport capacity exceeds supply over long time scales, then sediment depth will be effectively zero, although local, temporary patches of sediment can still exist.

All models explored in this study require the calculation of boundary shear stress (τ_b) for each model node, either for bedrock erosion estimates or for quantifying sediment transport capacity:

$$\tau_b = \rho g R S \tag{2}$$

where ρ is the density of water, g is gravitational acceleration, R is the hydraulic radius, and S is the bed slope. For a rectangular channel, the hydraulic radius is

$$R = \frac{A_c}{P} = \frac{WH}{W + 2H} \tag{3}$$

where A_c is the cross sectional area, P is the wetted perimeter, W is the channel width, and H is the flow depth. Flow depth is calculated using the conservation of mass for water discharge, Q_w:

$$Q_w = VA_c. \tag{4}$$

where the mean flow velocity, V, is estimated with Manning's equation:

$$V = \frac{1}{n} R^{\frac{2}{3}} S^{\frac{1}{2}} \tag{5}$$

where n is the Manning's roughness coefficient. For this study, I will assume that the channels are rectangular. Contrary to many studies, I make the wide channel assumption (i.e., $W \gg H$ and therefore $R = H$) only for scenarios in which the width to depth ratio (W/H) is greater than 5. For values of $W/H \leq 5$, the wide channel assumption is not used. I note that a W/H threshold of 5 is small given that for a rectangular channel, a W/H of 18 is required for H to be 90% of R; however, I find that the dynamics of the slope-width coupled modeled outlined below do not change significantly when using the wide channel assumption at $W/H > 5$ compared to model runs in which I raised the cutoff value. When the wide-channel assumption is not made, flow depth is estimated using Matlab's *fsolve* function which solves for a series of nonlinear equations (equations (3)–(5) in this case) using a least squares algorithm (Coleman & Li, 1996). When invoked (i.e., for narrow channels), this approach increases computational time. Future work should focus on understanding how cross-channel shape (e.g., nonrectangular channels) evolves in response to changes in sediment (Finnegan et al., 2007; Nelson & Seminara, 2011), base level, lithology, and water discharge.

2.1. Sediment Dynamics

For models accounting for the movement of sediment through the river system (Figure 2c), the conservation of sediment in the river channel is modeled using the Exner equation at each model node (Exner, 1920, 1925; Paola & Voller, 2005):

$$\frac{\partial h}{\partial t} = -\frac{1}{(1 - \lambda_p)} \frac{\partial q_s}{\partial x} \tag{6}$$

where q_s is sediment supply to and transported out of the local cell per unit width, x is distance downstream, and λ_p is sediment porosity, which is held constant for the modeled scenarios here.

Total sediment transport capacity, Q_t, is modeled using a modified Meyer-Peter Mueller equation (Meyer-Peter & Müller, 1948; Wong & Parker, 2006):

$$Q_t = 3.97 \rho_s W \left[\frac{\tau_b}{(\rho_s - \rho) g D} - \tau_c^* \right]^{3/2} D^{3/2} \sqrt{\frac{\rho_s - \rho}{\rho} g} \tag{7}$$

where ρ_s is the density of individual grains, τ_c^* is the Shields criterion (equal to 0.0495 [Wong & Parker, 2006] for all model runs here) and sets the critical shear stress for entrainment of a particle with b axis diameter of D. In this model, the bedload layer is transported across the entire width of the channel, W. Bedload grain size, D, is assumed to undergo downstream fining based on Sternberg's (1875) law:

$$D_{50} = D_0 e^{-a_s x} \tag{8}$$

where D_{50} is the median grain size at distance x from the headwaters, D_0 is the initial median grain size in first-order streams, and a_s is the downstream fining parameter. I limit fining to 5 mm if the model domain and Sternberg parameters would result in fining below this value.

Volumetric sediment supply to a river reach depends on three contributions: (1) the supply of sediment from the reach immediately upstream, (2) the supply of sediment from any tributaries draining into that particular reach, and (3) the supply of sediment from any hillslopes terminating directly into the reach.

While the model calculates the supply of sediment from the reach immediately upstream (Q_s), the sediment supply from local tributary and hillslope contributions must also be quantified. For all model runs, the flux of sediment supply from local contributions equal the local rate of river erosion averaged over the previous 10 kyr ($\bar{E}$):

$$Q_{Local} = \beta \bar{E} \partial A \tag{9}$$

where Q_{Local} is the local flux of sediment supply by tributary input and local hillslope processes, β is the fraction of that eroded material transported as bedload, and ∂A is the difference in drainage area between the upstream model node and the local channel. Because tributaries are not explicitly modeled, the drainage area change accounts for both tributary and hillslope contributions to increasing area that occur within a modeled river reach. The fraction of material moved as bedload, β, is poorly understood in many landscapes, with estimates ranging from 70 to 80% in headwater streams in landslide-dominated systems (Attal & Lavé, 2006) to $<$10% in systems lacking coarse sediment (Turowski et al., 2010). To avoid complications in interpreting model results, β is set to 30% for all runs.

2.2. Incision Processes

A number of processes are responsible for eroding bedrock (Whipple, Hancock, et al., 2000). As such, a number of different models have been described to capture the erosive potential of a river. Here I explore the implications of three different incision models: detachment-limited, sediment cover-shear stress, and saltation-abrasion. For each model, I will explore the implications of each of these models for a suite of different base level scenarios (i.e., rock uplift) to compare how slopes and width evolve for the different erosion mechanics assumptions.

2.2.1. Detachment-Limited Erosion

A common approach for bedrock detachment-limited models is the use of shear stress, τ_b (equation (2)), as a proxy for bedrock erosion potential (Howard & Kerby, 1983; Whipple & Tucker, 1999):

$$E = K {\tau_b}^a \tag{10}$$

where K is the erodibility controlled by lithology and a is an exponent that is usually between 1 and 2 (Whipple, Hancock, et al., 2000). I assume a = 1 for all modeled scenarios, which is equivalent to $n \approx 0.7$ in the common stream power equation (see below). In some cases, the equation uses a threshold to acknowledge that only discharges of a certain magnitude accomplish geomorphic work (Snyder et al., 2003; Tucker, 2004). A common argument for this use of a threshold is that sediment must become mobilized to expose bedrock and initiate erosion processes. Because I explicitly consider sediment mobility and bedrock exposure in four of the models presented below, I only consider a detachment-limited model without a threshold.

2.2.2. Sediment-Dependent Erosion

The effects of sediment on erosion can be quantified in a multitude of ways. As many bedrock rivers are covered with a blanket of alluvium that must be removed for erosion to occur, the development of a "cover" effect on bedrock erosion processes has proven useful to describing the relationship between sediment supply and bedrock erosion (Gasparini et al., 2007; Johnson et al., 2009; Kooi & Beaumont, 1994; Sklar & Dietrich, 2004; Turowski et al., 2007; Yanites & Tucker, 2010). A common approach is to consider the fraction of exposed bedrock, F, which will vary between 0 and 1 (Sklar & Dietrich, 2004), as a ratio between sediment supply and sediment transport capacity:

$$F = 1 - \frac{Q_s}{Q_t} \tag{11}$$

I use this bedrock exposure model for both the sediment cover-shear stress model and the saltation abrasion erosion model described below. I note that other formulations of the cover effect have been proposed (Turowski et al., 2007; Turowski & Hodge, 2017) that incorporate a probabilistic approach to sediment cover and future work should explore if such formulations predict fundamentally different behavior in river systems over landscape evolution time scales.

The sediment cover erosion model considered here is similar to the detachment-limited shear stress model described above but with an erosion capacity reduced by the fraction of bedrock that is covered and protected during erosional events in the system:

$$E = FK{\tau_b}^a \tag{12}$$

where a is an exponent that relates shear stress to process as in equation (10) above. Model parameterization is similar to detachment-limited (e.g., $a = 1$), but K is adjusted such that the initial and final profiles have relief on the order of 1–3 km for the initial profile to 1.5 to 5-km relief on the final profile. This approach ensures that the modeled profiles provide some context for real world landscapes.

Finally, the saltation abrasion model of Sklar and Dietrich (2004) models the erosion of rock as a function of the fraction of exposed rock, F, as well as the kinetic energy delivered to the bed by the impacts of saltating bedload. The model is formulated as follows:

$$E = V_i I_f F \tag{13}$$

where V_i is the volume of material removed per impact and I_f is the flux of particles per unit area (see equations (5) and (6) in Sklar and Dietrich, 2004 for full forms of V_i and I_f). The volume removed per impact depends on grain size, rock material properties and the vertical velocity of impacting sediment. The impact frequency is dependent on sediment supply per unit width, grain size, and hop length.

2.2.3. Classic Stream Power Erosion Rule and Analytical Scaling Relationships

The stream power erosion rule is the most commonly assumed river incision model. As such, I introduce the common usage and assumptions to facilitate comparison with the new modeling approach present here. An underlying assumption of the original derivations of the stream power equation (e.g., Howard & Kerby, 1983; Whipple & Tucker, 1999) is that erosion scales with stream power or shear stress (equation (10)). Assuming a wide channel and substituting equations (2)–(5), equation (10) can be rewritten:

$$E = K\left[\rho g\left(\frac{Q_w}{W}\right)^{3/5} S^{7/10}\right]^a \tag{14}$$

This equation is further simplified by assuming simple scaling between drainage area and both water discharge and channel width:

$$E = K_f A^m S^n \tag{15}$$

where K_f, m, and n are the "catch-alls" for all the coefficients and the exponent that are included in the derivation (Whipple & Tucker, 1999). Some derivations of the stream power erosion model do attempt to account for the effects of sediment (e.g., Gasparini et al., 2007); however, the nature of the equation limits geomorphic response to be accommodated solely by channel slope or by prescribed scaling between channel width, drainage area, and slope (Attal et al., 2008).

Channel steepness is a useful metric to quantify river morphology as it removes the influence of upstream contributing area, an empirically observed primary control on channel slope. It is based on the inverse relationship between channel slope and drainage area observed in many river channels (Flint, 1974):

$$S = k_s A^{-\theta} \tag{16}$$

where k_s is referred to as channel steepness and θ is the concavity. Because the units of channel steepness depend on theta, it is common to assume a constant theta value to compare rivers across a region (Wobus, Whipple, et al., 2006).

This general scaling relationship (equations (16) and (15)) is used to argue that channel steepness is reflective of the balance between rock-uplift rate, U_r (equation (1)), and erodbility, K_f (equation (15)). Assuming steady topography ($dz/dt = 0$ in equation (1)) and that equation (15) properly captures river dynamics in a tectonically active region, it can be shown that

$$k_s = \left(\frac{E}{K_f}\right)^{1/n} \tag{17}$$

This derivation does not allow for channel width to accommodate any of the erosion potential associated with changes in the erosion or rock-uplift rate; therefore, it provides a useful metric to compare the results of the model presented here with the classic stream power equation.

2.3. Channel Width

The finite-difference river profile model described in sections 2–2.2 incorporates an algorithm for dynamic channel width based on the assumption of river channel optimization (Nanson & Huang, 2008; Turowski et al., 2007; Yanites & Tucker, 2010). The model operates like a typical river profile model (Figure 2) but uses the state of river morphology, sediment supply, and water discharge to quantify channel narrowing or widening. Essentially, the constitutive equations described above are solved 3 times at each node, once for the current channel width configuration, once for a slightly (1%) wider channel, and once for a slightly (1%) narrower channel. The geometry that generates the greatest vertical erosion rate (if bedrock is exposed on the bed) or sediment transport rate (if bedrock is buried under an alluvial cover) dictates the direction (i.e., widening or narrowing) of channel width change but not the magnitude of channel width adjustment (see next paragraph). If the current width of a model time step generates the greatest incision, then width does not change. For example, consider the sediment cover model (equation (12)) with a relatively wide channel (e.g., $W/H > 20$) and little sediment cover (i.e., capacity greatly exceeds supply). Because the channel is wide, a narrower channel will generate a greater shear stress and thus erosion rate. In this case, the wide channel will limit any wall drag effects due to narrowing, and capacity will still significantly outpace supply, maintaining high bedrock exposure. With the model setup outlined above, this scenario will drive the system into a narrowing state. Alternatively, consider a relatively narrow channel (e.g., $W/H < 10$) that is overwhelmed with sediment and bedrock exposure is rare. Because of the importance of the width in controlling transport capacity (equation (7)), a slightly wider channel can result in more bedrock exposure, thus increasing the rate of vertical incision (whereas a narrower channel would further reduce exposure). In this case of a relatively narrow channel, the model will enter a state of widening.

The magnitude of channel widening (+) or narrowing (−) is dependent on the current river shear stress and a channel adjustment factor (k_w):

$$W = W_i \pm k_w \tau \tag{18}$$

where W_i is the initial width and W is the model updated width. The channel adjustment parameter, k_w, is chosen such that the rate of channel width change is capable of producing multiple river strath terraces over an ~10^3 to 10^4-year time scale with a reasonable variation in sediment supply (or water discharge for the detachment-limited runs). This is consistent with the observation that many tectonically active landscapes contain at least one, and in many instances multiple, Holocene river terraces (Brocard & van der Van Der Beek, 2006; Bufe et al., 2016; Lavé & Avouac, 2001; Pazzaglia et al., 1998; Yanites et al., 2010). I note that this parameter could be calibrated for specific field sites containing dated strath terraces, provided the straths are planed by channel widening and abandoned by narrowing/incision (Bull, 1990) and not due to autogenic processes such as meandering (Finnegan & Dietrich, 2011; Limaye & Lamb, 2016). This could work for lateral migration and valley widening (Hancock & Anderson, 2002; Langston & Tucker, 2018; Pazzaglia et al., 1998) as well by quantifying a lateral planation rate during times of reduced vertical incision.

Although this is an ad hoc approach to driving channel width change, there are physical arguments that justify such an approach. Stochastic events such as scour events and bank failure generate a range of channel width scenarios for any given river reach. Through the range of such events and geometries, the river channel will experience a range of vertical erosion rates; however, the geometry that drives the greatest magnitude of vertical erosion over time will entrench the channel more than the other scenarios. Thus, when averaged over time, the channel will tend toward being entrenched (i.e., in confined bedrock banks) in a geometric configuration that leads to the greatest vertical incision. Whereas skepticism of this justification is to be expected, I will show that the behavior of width using this approach is consistent with observations of how channels

respond to changes in base level and water/sediment discharge in natural river systems while limiting the number of additional parameters.

Borrowing from the same origin as the term "channel steepness" and the term "normalized wideness index" from Allen et al. (2013), I introduce a term called channel wideness. This is a metric that allows the comparison of channel widths relative to the contributing drainage area and is based on the relationship between upstream contributing area and channel width observed in natural settings (Allen et al., 2013; Montgomery & Gran, 2001; Whittaker et al., 2007b; Yanites et al., 2010) and predicted by models (Finnegan et al., 2005; Nelson & Seminara, 2011; Turowski et al., 2007; Wobus, Tucker, & Anderson, 2006; Yanites & Tucker, 2010):

$$W = k_b A^b \tag{19}$$

where b is an exponent that relates drainage area and width and k_b is the coefficient that I call channel wideness. Calculating empirical and modeled values of k_b allows a comparison of channel width among different basins and along channel paths as it normalizes for upstream contributing drainage area. This metric will be important for comparing the model results to quantify the magnitude and direction of channel width changes in response to changes in tectonic uplift.

2.4. Parameterization and Initiation

Many model parameters vary as a function of distance downstream. Here I present the relationships used in this modeling. These values are held constant through the model runs, except where explicitly stated. I note that future work that considers different functions or relationships that also depend on time or local erosion rate could reveal rich model behavior that may better explain natural observations in channel morphology and sediment cover.

Water discharge, Q_w, is assumed to scale with drainage area (A):

$$Q_w = k_Q A^c \tag{20}$$

where c is an exponent set to 1 for this study. With $c = 1$, the coefficient, k_Q, effectively becomes an upstream average runoff term. Drainage area is set using Hack's law which relates drainage area to distance downstream (Hack, 1957):

$$A = C_h x^{H_e} \tag{21}$$

where $C_h = 1$ and $H_e = 1.8$ are coefficients and exponents often empirically derived.

The model is initialized with a channel width that is a function of water discharge:

$$W_0 = k_{wq} {Q_w}^b \tag{22}$$

where the coefficient k_{wq} is 2 and b is set to 0.5 for this study. Once channel width is initialized, these parameters do not further influence model behavior. Table 1 lists other parameter values such as channel roughness (n), fraction of sediment supply transported as bedload (β), and headwater grain size (D_0).

The initial rock-uplift rate (U_r)is set at 0.5 mm/yr along a 205-km long river profile. To avoid any complexity with debris flow-fluvial transition, the modeling begins at 5 km from the drainage divide (with one exception explained below) for a total of a 200-km-long model run. For the sediment transport models, the sediment cover term is initialized at $F = 1$. The forward model operates in the following manner: (1) The landscape is uplifted according to the rock-uplift rate; (2) slopes along the profile are calculated; (3) shear stress is calculated for the current channel morphology as well as for a slightly wider and narrower channel; (4) starting at the upstream node, sediment supply and transport capacity for the current time step, as well as slightly wider/narrower channel, is calculated for each node. Sediment is transported to the downstream node for the current channel geometry (Step 4 is ignored in the runs that do not include the effects of sediment); (5) erosion rate along the profile is calculated using the current time step channel morphology; and finally, (6) elevation and channel width values are updated according the vertical erosion or channel width adjustment equations described above. The initial system is run to steady state such that channel elevation, slope, and width are effectively unchanging (<0.5% change over 10 kyr). The models incorporating sediment

Table 1
Parameters for Different Modeled Suites

Parameter	Units	Detachment-limited	Sediment cover (detachment-limited)	Sediment cover (exposure-limited)	Saltation-abrasion (tool-limited)	Saltation-abrasion (exposure-limited)
Shear stress erosion parameters						
K	m^2 s/kg	1.0E − 04	3.0E − 05	3.0E − 03	n/a	n/a
a	—	1	1	1	n/a	n/a
Channel adjustment coefficient						
k_w	m^2 s/kg	2.0E − 03	2.0E − 04	2.0E − 04	2.0E − 04	2.0E − 04
Sediment parameters						
a_s	1/m	n/a	2.0E − 05	1.0E − 05	2.0E − 05	2.0E − 05
D_0	m	n/a	0.1	0.2	0.3	0.3
D_{min}	m	n/a	0.005	0.005	0.005	0.005
β	—	n/a	0.3	0.3	0.3	0.3
λ	—	n/a	0.2	0.2	0.2	0.2
τ_c^*	—	n/a	0.0495	0.0495	0.0495	0.0495
ρ_s	kg/m^3	n/a	2,650	2,650	2,650	2,650
Initiation parameters						
n (Manning's n)	$s\ m^{-1/3}$	0.04	0.04	0.04	0.04	0.04
b	—	0.5	0.5	0.5	0.5	0.5
k_{wq}	$s^b\ m^{1-3b}$	2	2	2	2	2
k_Q	m/s	1.0E − 07	1.0E − 07	1.0E − 07	1.0E − 07	1.0E − 07
Model setup						
dt	yr	10	1	1	1	1
Timing of increase in rock-uplift	My	2	5	5	5	5
dx	km	2	2	2	2	2
Saltation-abrasion parameters (see Sklar & Dietrich, 2004 for full model formulation)						
Y (Young's elastic modulus)	Pa	n/a	n/a	n/a	5.0E + 10	5.0E + 10
σ_T (tensile strength)	Pa	n/a	n/a	n/a	1.4E + 07	7.0E + 06
kv (rock resistance parameter)	—	n/a	n/a	n/a	1.0E + 06	1.0E + 06

transport require short time steps, especially during large transient changes (see section 3 below). The initial steady state profiles set the stage for the numerical experiments described below.

3. Numerical Experiments

Interactions among channel width, sediment, and channel slope on river profile dynamics are explored by running a suite of numerical experiments for each of the three incision models described above: detachment-limited, sediment cover erosion, and saltation-abrasion. After the initial steady state longitudinal profile and channel width pattern is established, an instantaneous increase in rock uplift is applied to the entire profile (i.e., a uniform increase in rock uplift) and the system evolves to a new steady state. For each case, I increase the rock-uplift rate on the initial steady state profile by 2, 3, 5, 10, and 20-fold, generating five separate transient model runs for each erosion approximation. I refer to the runs that ignore the effects of sediment as the bedrock detachment-limited (BR-DL) runs. For the sediment cover erosion model, I run two suites, one that is parameterized (Table 1) with high bedrock exposure ($F > 0.2$) in the initial steady state profile, and one that is parameterized with low bedrock exposure ($F < 0.05$), as the transient response is distinctly different between these endmembers. I refer to these suites as "sediment cover detachment-limited" (SC-DL) and "sediment cover exposure-limited" (SC-EL), respectively. For saltation-abrasion, I also run two suites of experiments intended to explore the range of "saltation abrasion exposure-limited" (SA-EL) to "saltation abrasion tool-limited" (SA-TL) scenarios. The tool-limited run is accomplished by doubling the rock tensile strength, which reduces the volume removed per impact (V_i) and causes a more tool-limited model behavior (Table 1). I will compare the results of these model runs systematically to understand differences in model behavior and the implications of the interaction of channel geometry, sediment transport, and profile development.

I focus the analysis on the sensitivity of each model to increases in rock uplift. The erosion and sediment parameters (Table 1) were selected to illustrate a range of behaviors that emerge over fluvial relief magnitudes consistent with modern orogens (e.g., 1–5 km) among the different vertical erosion models considered. In order to accomplish this, differences in sediment characteristics (e.g., grain size) were parameterized to drive exposure versus detachment/tool limited scenarios. I note that variations in sediment supply could cause

these regime shifts; however, sediment supply is ultimately driven by rock uplift, the variable that is driving transience response. Therefore, changes in rock uplift will change sediment supply once the river adjusts to the new uplift rate. Differences in sediment characteristics are therefore used to drive regime differences in the initial models. For these reasons, I urge the reader to consider the predictions of each suite of models as representative of different regimes that emerge in the different models. A broad range of model behaviors is certainly possible if one considered a full sensitivity to the range of all possible parameter combinations. Future work should consider how the different parameters influence the time scale and style of adjustment for each of the erosion models presented.

4. Results

4.1. Bedrock Detachment-Limited (BR-DL)

The steady state river profiles for the bedrock detachment-limited runs reproduce the basic characteristics found in previous studies exploring channel width, erosion, and slope. Such relationships include constant *W*/*H* ratios and inverse scaling between width and erosion rate (Finnegan et al., 2005; Wobus, Tucker, & Anderson, 2006; Yanites & Tucker, 2010). The consistency between the *W*/*H* values generated in the BR-DL models here (3.3–3.4, Table 2) and the W/H predicted by the Wobus, Tucker, and Anderson (2006) model, which range between 3.06 and 3.54, provides further evidence that this approach can capture general dynamics of more sophisticated modeling approaches.

Incorporating a dynamic channel width in river profile models lowers the sensitivity of river profile response to changes in rock uplift compared to models that only allow slope adjustments (Figure 3). To compare how the increase in rock uplift influences the overall topography, I calculate the change in steepness (k_s) of the river profile for each incremental increase in rock uplift. In Figure 3, I plot the change in steepness for a given change in the rock-uplift rate for the modeled scenarios as well as for the prediction from the 1-D stream power equation with no dynamic channel width (Whipple & Tucker, 1999). For a doubling of the rock-uplift rate, the modeled profiles respond by increasing average channel steepness by 2.3. For no dynamic width cases (and an equivalent exponent of $n = 0.7$ on channel slope), steepness is expected to increase by 2.7 (equation (17)). The difference in slope response between dynamic width and static width grows with increasing rock uplift. For a 20-fold increase in rock-uplift rate, the dynamic width model predicts 38.6-fold greater channel steepness, whereas the static width predicts a 72.2-fold increase (Figure 3a).

For the BR-DL model, the increase in rock-uplift rate results in narrower channels, with more narrowing associated with a greater change in rock uplift (Figure 3b). Equations (1) and (10) require that for steady state channels, the fluvial shear stress is equal to U/K. The implication of the results in the BR-DL case is that adjustments in channel width can absorb some of the topographic imprint of an increase in rock-uplift rate, resulting in less of a slope adjustment to reach steady state. A general conclusion of the models presented here (Figure 3) is that the partitioning between slope and width adjustment depends on the rock-uplift rate.

The advantage of this modeling approach over the steady state analytical solution (e.g., Yanites & Tucker, 2010) is that it provides information on the transient nature of the response. This allows a more careful consideration of how the system responds to changes in forcings for these different erosion mechanics and parameterizations. To explore the transience in slope and width in the detachment-limited case, I focus the analysis on the fivefold increase in rock uplift runs and note that the other scenarios behave similarly but with different magnitudes. Channel narrowing accompanies a migrating knickzone as the river profile adjusts to the increase in rock uplift (Figures 4 and 5). Following the passage of the knickzone, the river remains narrow, a key model result distinguishing it from other model formulations (see below). The *W*/*H* ratio initially increases at the downstream location as the knickzone arrives (Figure 5c). This is because flow velocity increases (and flow depth decreases) in response to the increased slope, but channel narrowing has yet to catch up because the channels are wide at the downstream reaches and require more time to fully adjust the cross-channel geometry. It is clear in Figure 5c that channel narrowing is occurring, but the initial narrowing effects on the *W*/*H* ratio are outweighed by the channel velocity changes. For system changes driven by bottom up processes (e.g., changes in base level due to changes in the rock-uplift rate), the slope has to change first (even if just by a minor amount) in order to drive the regime into a state of narrowing. Other than the short-lived lag between slope and width changes at the downstream reaches (Figure 5c), channel width and slope are tightly coupled in the BR-DL models. This tight coupling has also been predicted by other

Table 2
General Morphological Results for the Fivefold Increase in Rock-Uplift

Run	Run abbreviation	k_b (b = 0.45)		k_s (θ = −0.5)		W/H	
		Initial value	After 5× increase	Initial value	After 5× increase	Initial value	After 5× increase
Bedrock detachment-limited	BR-DL	0.0009	0.0006	67	458	3.3	3.4
Sediment cover, detachment-limited	SC-DL	0.003	0.002	161	701	24.5	20.2
Sediment cover, exposure-limited	SC-EL	0.002	0.003	380	1,048	17.7	47.2
Saltation-abrasion, tool-limited	SA-TL	0.0023	0.002	258	701	18.3	19.1
Saltation-abrasion, exposure limited	SA-EL	0.0029	0.0033	244	595	31.7	49.4

models incorporating channel width adjustment into a detachment-limited framework for modeling river dynamics (Attal et al., 2008; Finnegan et al., 2005; Wobus, Tucker, & Anderson, 2006).

4.2. Sediment Cover

In general, incorporating a sediment cover term generates wider channels for a given discharge than the BR-DL model. This result is consistent with previous work considering the feedbacks among erosion, slope,

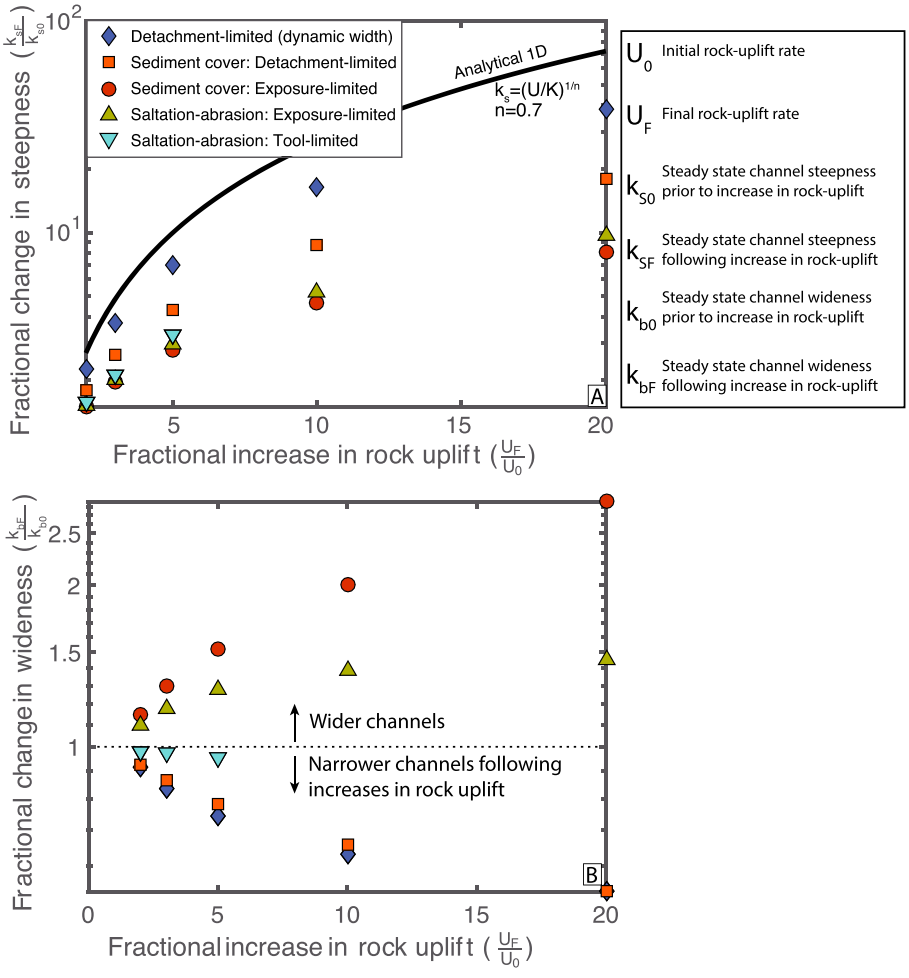

Figure 3. Changes in steady state mean channel (a) steepness and (b) wideness for a given change in rock-uplift. Five different modeled scenarios each experiencing 2, 3, 5, 10, and 20-fold increases in rock-uplift are depicted with symbols. Channel steepness prediction based on the 1-D stream power model is shown with the bold black line. For the channel wideness plot, the dotted horizontal line depicts no change in width. Points below the line show overall narrowing along the river profile, while points above the line show overall widening. Note that these points represent the average change along the profile. In some specific cases, both narrowing and widening occurred in different parts of the basin. This narrowing versus widening is illustrated and discussed later in the text. The saltation-abrasion tool limited runs (cyan down-pointing triangles) resulted in fluvial "hanging valleys" as rock-uplift outpaced the ability for tools to erode (Crosby et al., 2007; Gasparini et al., 2007) in the 10 and 20-fold increase in rock-uplift runs.

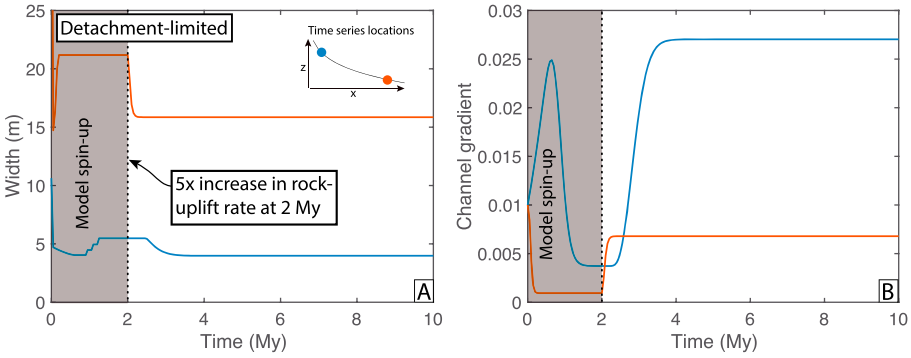

Figure 4. Time series of the BR-DL run showing the evolution of (a) channel width and (b) slope for two locations, 8 km upstream of the outlet (orange) and 8 km downstream of the headwaters (blue), for the fivefold increase in the rock-uplift rate. The gray area is the model spin-up during which the river profile and width equilibrate to the 0.5-mm/yr initial rock-uplift rate. For this modeled scenario, channel narrowing and steepening are tightly coupled.

and width for steady state channels (Johnson et al., 2009; Turowski et al., 2007; Yanites & Tucker, 2010). Width-to-depth ratios among the sediment model runs are typically 5–10× larger than the BR-DL runs (Table 2).

4.2.1. Sediment Cover Detachment-Limited (SC-DL)

Changes in channel steepness in the sediment cover detachment-limited runs are similar to the BR-DL run but exhibit less sensitivity to changes in rock uplift. For example, a twofold change in rock uplift results in a 1.8-fold increase in channel steepness (Figure 3a), whereas the 20-fold increase in rock uplift only generates an 18-fold increase in steepness (compared to a 38.6-fold increase for the BL-DL and a 72.2-fold increase for the 1-D analytical model). The lower sensitivity occurs because an increase in shear stress generates both increased detachment capacity (τ) and higher bedrock exposure (F) (equation (7)). This "double-whammy" effect of an increase in shear stress, enhancing both detachment capacity and bedrock exposure, leads to the lower sensitivity of the stream profile to rock uplift than in the pure BR-DL case.

In the case of a fivefold increase in rock-uplift rate for the SC-DL run, channel narrowing accompanies the migration of the knickzone as in the BR-DL model (Figures 6a and 6b and 7a and 7b). Following the passage of the knickzone, there is a slight widening in the river (Figure 6a). This increase in width is the system responding to the increase in sediment supply as the transient incision migrates upstream.

A number of factors influence the pattern of exposed bedrock along the channel (Figure 8) such as the downstream distribution of grain size (see equations (7), (8), and (10)); however, the transient channel response disrupts these patterns. Bedrock exposure initially increases in the downstream reaches as the increase in slope associated with the arrival of the knickzone increases capacity (Figures 7d and 8). As sediment supply increases due to the migrating knickzone, exposure decreases slightly but remains above the preuplift value. In the upstream reaches, exposure monotonically increases as the knickzone arrives. This increase in exposure persists even when the increase in sediment supply has propagated up through the entire system (Figure 8).

4.2.2. Sediment Cover Exposure Limited (SC-EL)

In the sediment cover exposure-limited scenario (SC-EL), there was even less sensitivity to a change in rock uplift (Figure 3a). A 20-fold increase in rock uplift only generated 8.1-fold increase in channel steepness. This lower sensitivity occurred even though the final channel configuration was wider than prior to the increase in uplift (Figure 3b). This nonintuitive result of a wider channel with greater uplift occurs when the system becomes bedrock exposure-limited. As the transient signal propagates upstream increasing hillslope supply, the river system experiences full bedrock cover (i.e., $F = 0$). The system initially responds by steepening because $U > E$ (and $E = 0$). As the system is dominated by sediment transport efficiency at this point, a wider channel becomes more efficient at conveying the bedload discharge because of the width of active bedload transport (i.e., the W in the numerator of equation (7)) outweighs the reduction in excess shear stress due to a wider channel. Therefore, a slight steepening accompanied by widening is able to increase bedrock exposure enough to allow for erosion to equal rock uplift with the higher sediment supply. The result is consistent, as expected given the model assumptions, with steady state analytical predictions of the sediment cover erosion model (Yanites & Tucker, 2010). I note that this increase in sediment supply occurs after the transient increase in erosion has propagated upstream.

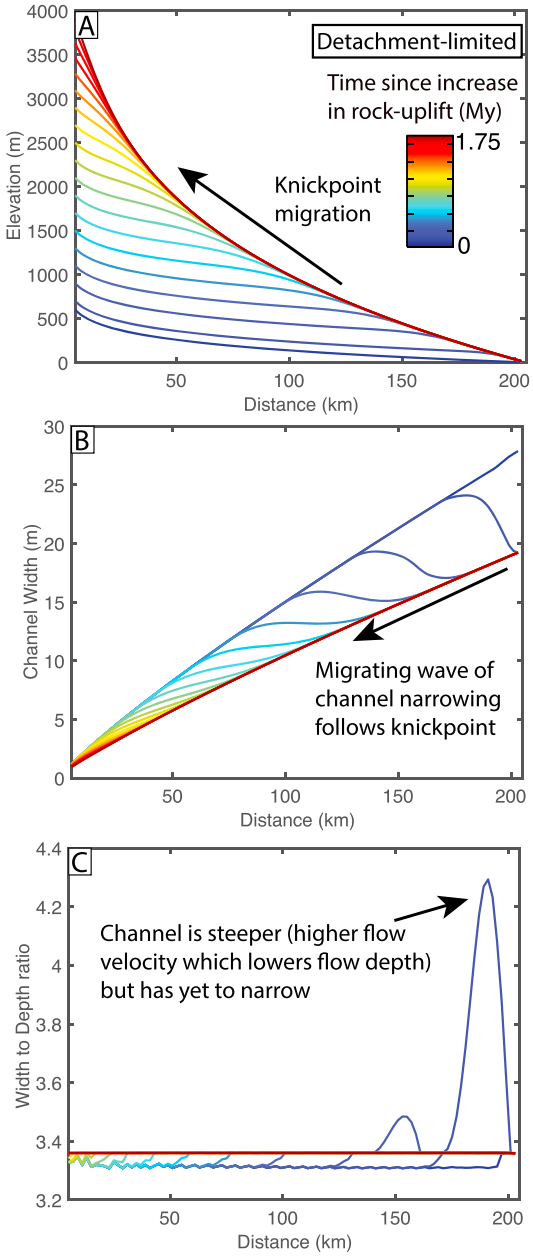

Figure 5. Evolution of the (a) channel profile, (b) width, and (c) *W*/*H* ratio along the river profile for the BR-DL run with a fivefold increase in rock uplift. Profiles are colored by time with cool colors representing early in the transience (the lowest profile is the preincrease steady state profile).

In the transient response to a fivefold increase in rock uplift, slope adjustment starts prior to changes in channel width (Figures 6c and 6d and 7e and 7f). In the downstream reach, this time difference is quite small (<10 kyr) because the transience travels rapidly at first; however, in the upstream reaches, this time difference is larger (~50 kyr) as the transient signal slows down as it approaches the headwaters. This initial increase in slope is the response to the increase in base level lowering from rock uplift but prior to any increase in sediment supply. The subsequent increase in width is the main morphologic response to the increase in sediment supply as the transient incision signal migrates upstream. The continued steepening and widening (Figures 6c and 6d and 7e–7g) is the continued response as the system erodes at the rate of higher rock uplift while adjusting to the increasing sediment supply, increasing sediment transport capacity (Figure 7h), as the transient signal propagates through the landscape.

4.3. Saltation-Abrasion

The altation-abrasion model behaves similarly to the sediment cover model. Channel steepness is impacted by rock uplift in a similar manner in that the model run limited by the exposure of bedrock (SA-EL) is less sensitive to rock uplift than the tool-limited (SA-TL) run, which was modeled by increasing the resistance to abrasion. The SA-EL run experiences channel steepening followed by widening as the increased incision and sediment supply migrates upstream. Channel width also increases in response to higher rock-uplift rates for the SA-EL runs though to a lesser extent than in the exposure-limited sediment cover (SC-EL) model (Figure 3b) for the parameter combinations used here (Table 1). Channel steepness in the SA-TL (tool-limited) run is more sensitive to rock uplift than in the SA-EL runs but still less sensitive than the full detachment-limited models (Figure 3a). The SA-TL runs show little sensitivity of channel width to rock uplift (Figure 3b). For the 10-fold and 20-fold increases in rock uplift, "hanging valleys" develop well downstream of the headwaters as rock uplift outpaces the ability for tools to erode bedrock (e.g., Crosby et al., 2007). Therefore, I do not plot them on Figure 3 as they never achieve steady state. This phenomenon also occurs in the upper 15 km of the fivefold increase in rock uplift. After recognizing this, I reran the models for twofold, threefold, and fivefold increases in rock-uplift rate for the tool-limited runs starting at a downstream distance of 15 km. This ensures that the area upstream of 15 km erodes and supplies sediment at the rock-uplift rate, which would not happen if the model develops a hanging valley.

The transient evolution of channel width and slope for the SA-EL run behaves similarly to the SC-EL model, while the SA-TL model evolved similarly to the SC-DL model (compare Figures 6 and 7 and 9 and 10). The additional dependence on sediment transport in the saltation-abrasion models compared to the sediment cover models did cause some noticeable differences. For example, there is a clear variable response to the upstream propagating increase in sediment supply that prevents any clear monotonic changes in channel width (e.g., the variability observed in Figure 10b). In the fivefold increase in rock uplift for the SA-TL run, channel narrowing accompanies the migration of the knickzone as in the BR-DL and SC-DL models. Following the passage of the knickzone, there is a slight widening in the river in the downstream reaches (Figure 9c). In the upstream reaches, the channel becomes wider than the preuplift river. This increase in width is the system responding to the increase in sediment supply as the transient incision migrates upstream and generates greater sediment supply. Such trade-offs between channel narrowing

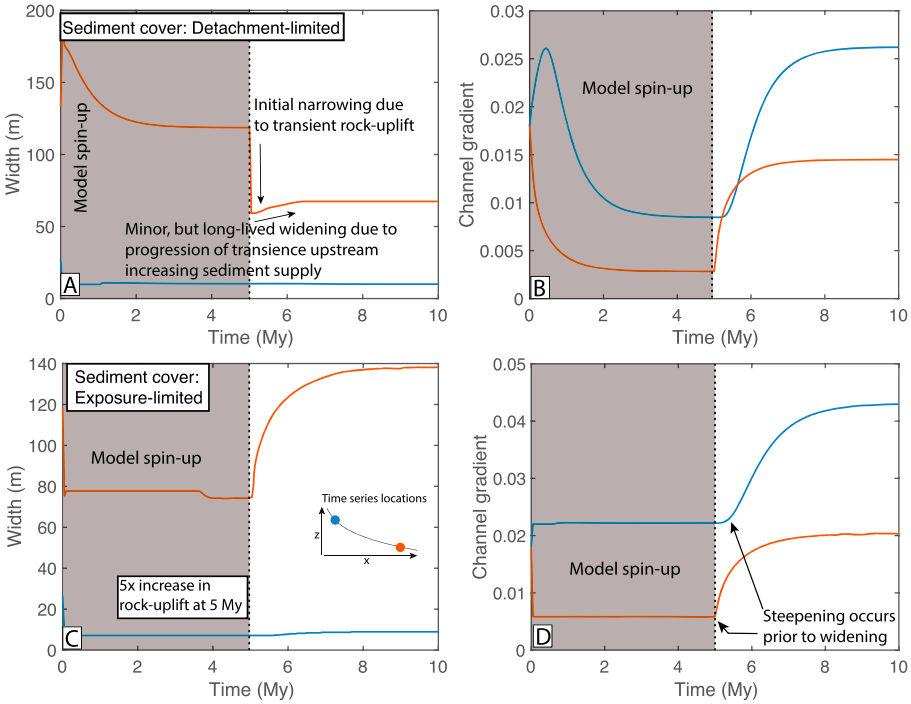

Figure 6. Time series of the sediment cover runs showing the evolution of (a and c) channel width and (b and d) slope for two locations, 8 km upstream of the outlet (orange) and 8 km downstream of the headwaters (blue). (a) and (b) show the time series for the SC-DL runs, which behaved similarly to the detachment-limited runs (Figure 4). (c) and (d) show the time series for the SC-EL runs. The gray area is the model spin-up during which the river profile and width equilibrate to the 0.5-mm/yr initial rock-uplift rate. For the SC-EL runs, the lag indicated on the plot between steepening and widening is ~50 kyr for the downstream reach and ~100 kyr for the upstream reach. Also, note the contrasting behavior in channel width (narrowing in a and widening in c) compared to channel gradient evolution (b and d).

versus widening depend on a multitude of factors such as the parameterization of Sternberg's Law (equation (8)) and the proportion of sediment supply that gets transported as bedload (β in equation (9)). Future work exploring the interactions of these parameters along the path of a particular river corridor will be a fruitful exercise in further understanding the modeling approach described here.

5. Discussion

The results presented above have a number of implications including how to appropriately model river systems, predict topographic response to tectonic and climatic change, and interpret patterns of channel width and slope in transient river systems. The first part of the discussion focuses on the implications of incorporating channel width and sediment into the transient evolution of river profile models. Next, I discuss how the model can be used to help interpret channel morphology in regions with spatial and/or temporal changes in rock uplift. This includes potential field applications of this approach such as how patterns in both width and slope can be used to provide insight on the dominant physical mechanisms controlling channel evolution. Finally, I point out some implications for climate change on orogen relief based on modeling results presented here.

5.1. Model Implications

5.1.1. Implications of Dynamic Width

The model results show that dynamic channel width can significantly influence river profiles and, ultimately, the topographic response to climate and tectonic changes at an orogen scale. This is evident even for simple, detachment-limited cases as the channel steepness difference between dynamic and static width in response to a change in rock uplift can differ by almost 100% (38 versus 72-fold increase in steepness for a 20-fold increase in rock uplift, Figure 3). As channel profiles control the relief structure of active orogens, such acknowledgement and quantification of the limitations of 1-D river models is necessary when applying these models to real landscapes. In a careful field campaign in which one calibrates the stream power model,

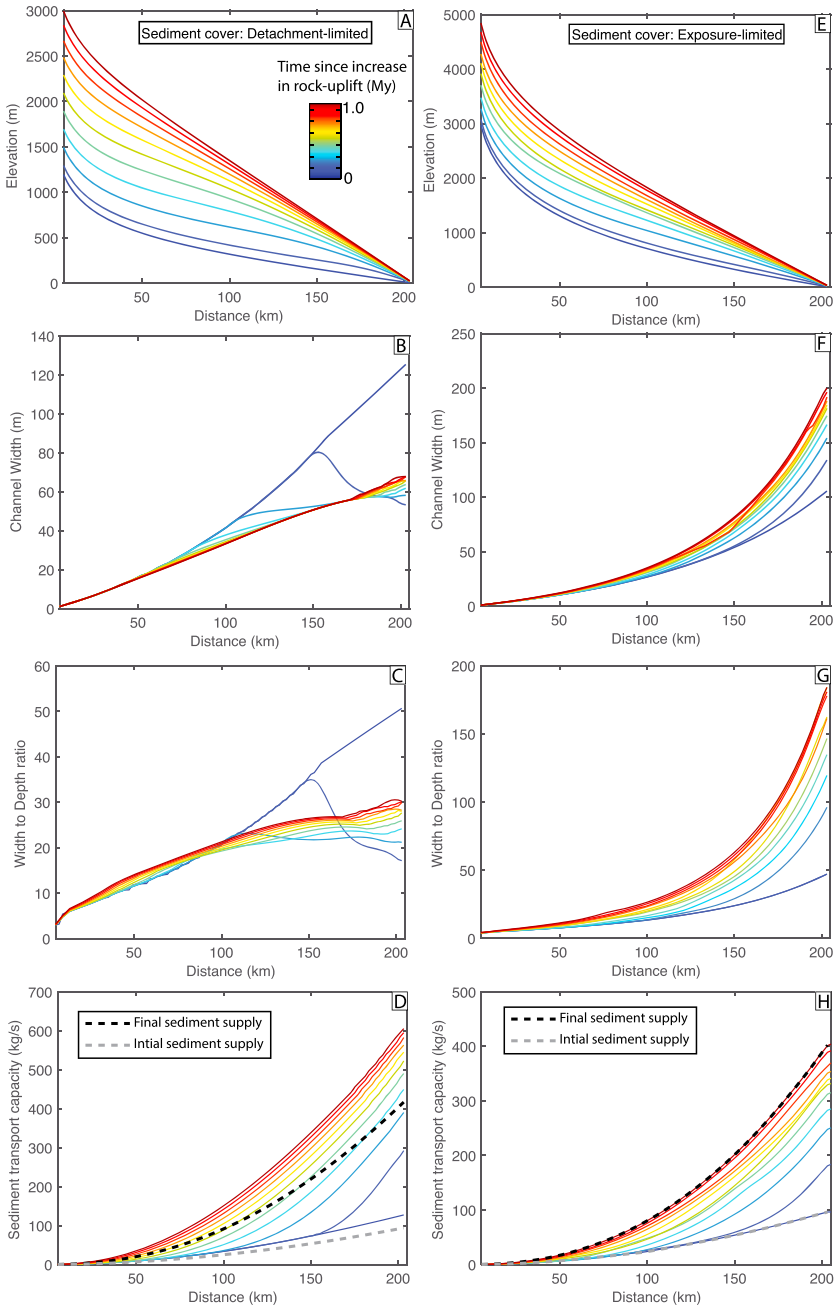

Figure 7. Evolution of the (a and e) channel profile, (b and f) width, (c and g) *W*/*H* ratio, and (d and h) sediment transport capacity along the river profile for the sediment cover runs with a fivefold increase in rock uplift. Profiles are colored by time with cool colors representing early in the transience (the lowest profile is the preincrease steady state profile). (a)–(d) represent the SC-DL run, and (e)–(h) show the SC-EL run.

impacts of a dynamic channel width could be accounted for in the coefficients (i.e., "K_f") and exponents ("*m*" and "*n*") of the equation if the variations are systematic with drainage area. However, in cases in which the equation is applied without a priori information such as inversion approaches, the 1-D model may over predict the topographic response to changes in the driving forces (e.g., uplift) because it cannot account for part of the signal being "absorbed" by changes in channel width (Attal et al., 2008).

5.1.2. Implications of Sediment Transport

The BR-DL model is the most sensitive to changes in rock uplift, predicting the greatest change in relief for an increase in rock uplift (Figure 3). If the sediment transport-dependent models more appropriately capture the relevant physics of the river system, then the use of the detachment-limited model will overestimate the

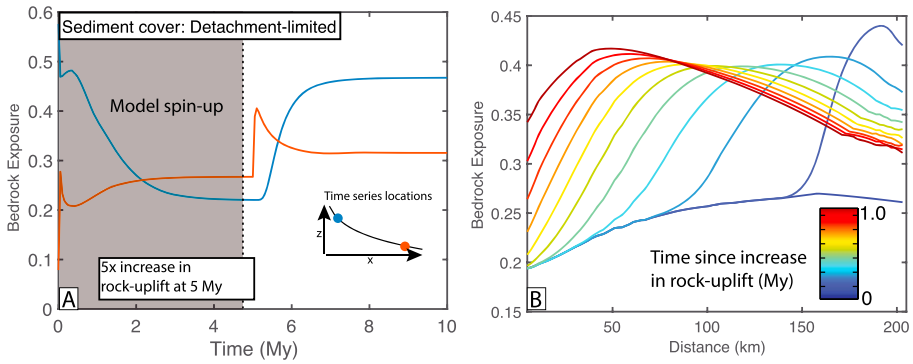

Figure 8. (a) Time series and (b) spatial pattern of the bedrock exposure for the SC-DL run with a fivefold increase in rock-uplift. Increases in shear stress increase bedrock exposure as well as erosion potential, leading to a lower sensitivity between topographic adjustment and rock-uplift.

topographic response to tectonics in a model (or underestimate the tectonic forcing if applying the model in a field setting; Cowie et al., 2008). One reason for the reduced topographic response in the sediment dependent models is that channel width and slope changes increase both the erosion potential (i.e., shear stress) as well as the frequency of bedrock exposure. This "double-whammy" effect results in any change in shear stress impacting two facets of the geomorphic system, sediment transport capacity, and erosion/detachment potential. In other words, in the detachment-limited model, as parameterized here, a doubling of shear stress doubles the erosion rate (equation (10)); however, in the sediment cover and saltation abrasion models, a twofold increase in shear stress can more than double the erosion rate.

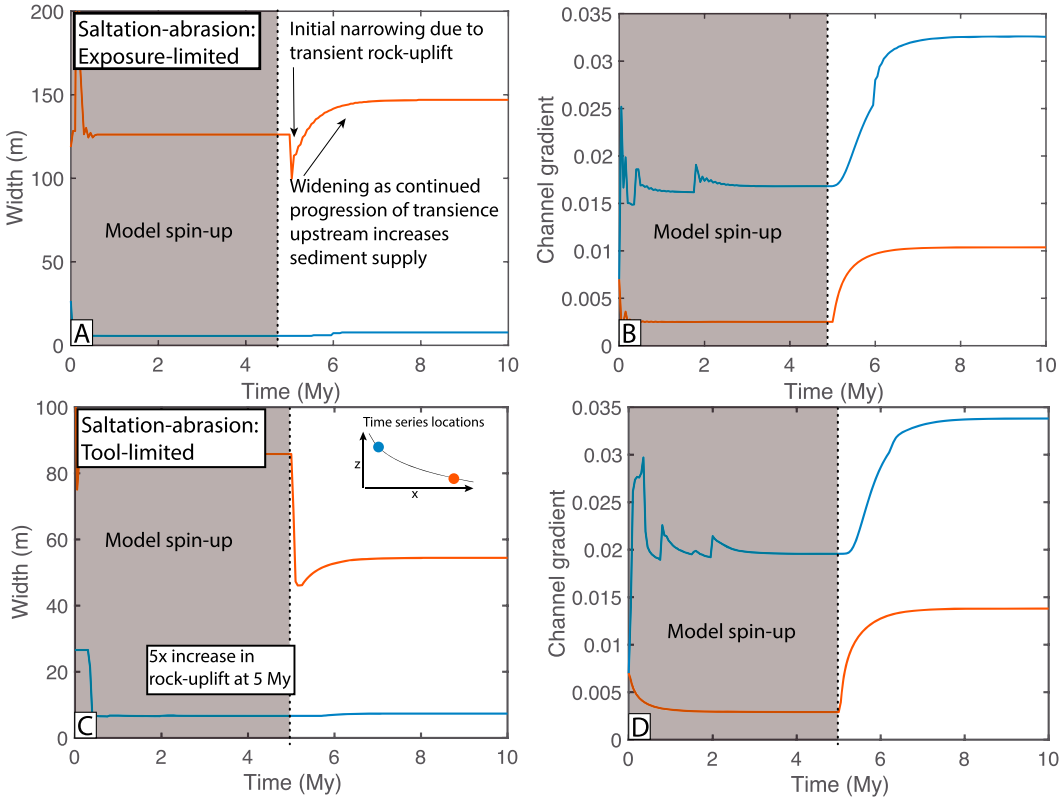

Figure 9. Time series of the saltation-abrasion runs showing the evolution of (a and c) channel width and (b and d) slope for two locations, 8 km upstream of the outlet (orange) and 8 km downstream of the headwaters (blue). (a) and (b) show the time series for the SA-EL runs, which behaved similarly to the SC-EL runs (Figure 6). (c) and (d) show the time series for the SA-TL runs parameterized by modeling harder rock (i.e., greater tensile strength). The gray area is the model spin-up associated with coming into equilibrium of the 0.5-mm/yr initial rock-uplift rate. Note the contrasting behavior in channel width (widening in a and narrowing in c) compared to channel gradient evolution (b and d).

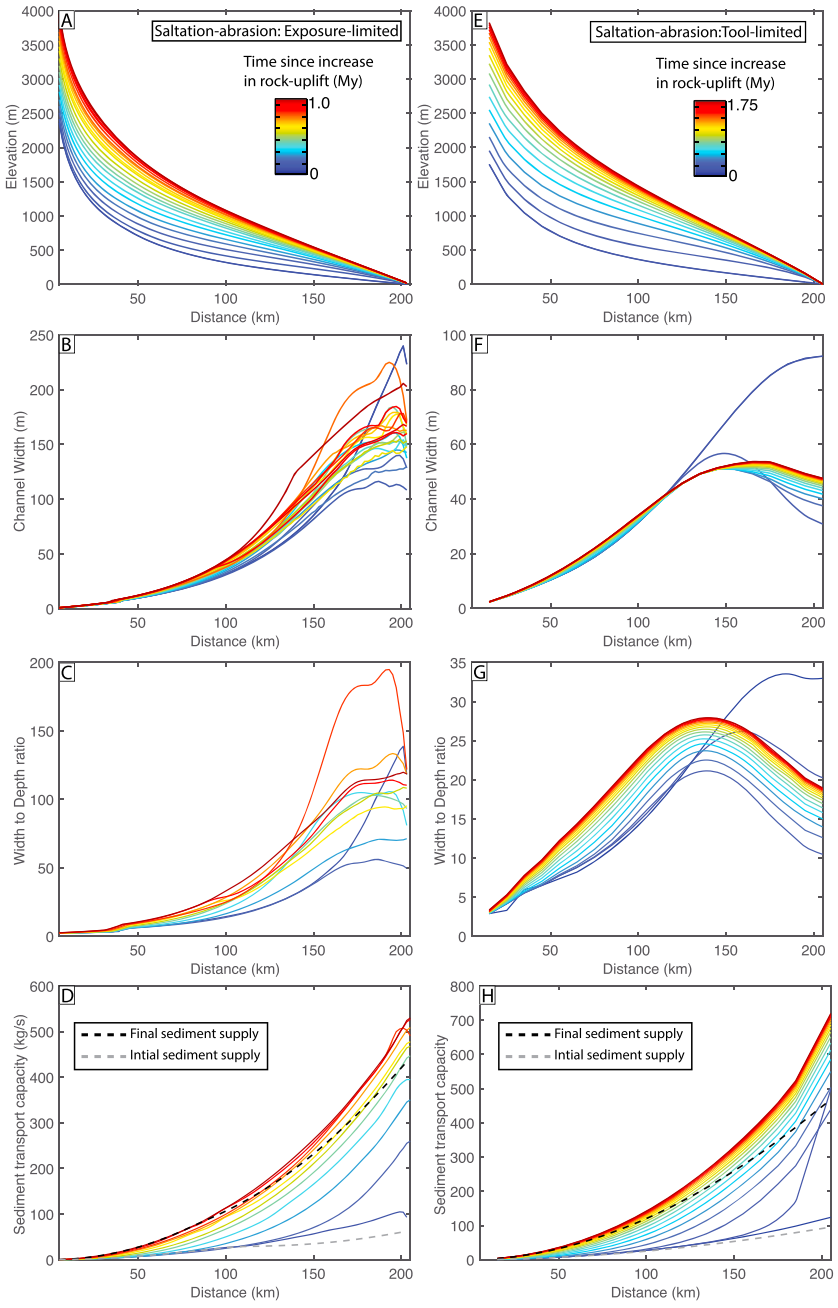

Figure 10. Evolution of the (a and e) channel profile, (b and f) width, (c and g) *W*/*H* ratio, and (d and h) sediment transport capacity along the river profile for the saltation-abrasion runs with a fivefold increase in rock uplift. Profiles are colored by time with cool colors representing early in the transience (the lowest profile is the preincrease steady state profile). (a)–(d) represent the SA-EL run, and (e)–(h) show the SA-TL run. The upper reaches of (e)–(h) were not modeled because of the development of hanging valleys (see text for explanation).

Consider the sediment cover model where a doubling of shear stress will increase bedrock detachment by twofold and sediment transport capacity by up to ~2.8-fold ($2^{3/2}$ when $\tau_b >> \tau_c$), assuming there is no change in channel width (recall *W* in equation (7)). This increases bedrock exposure by an equivalent factor, resulting in a potential ~5.7-fold increase in erosion rate due to a doubling of shear stress.

When sediment clogs the system and erosion dynamics are dictated by the ability for the system to expose bedrock, the river responds in a more transport-limited manner (Johnson et al., 2009; Lague, 2010; Turowski et al., 2007; Yanites & Tucker, 2010). Such systems respond to an increase in rock uplift by widening and steepening (Figures 3, 6, and 7e and 7f). This behavior emerges because in equation (7), a wider and

steeper channel will transport more sediment than one with the same shear stress but narrower and with a gentler slope (e.g., Yanites & Tucker, 2010).I note that these model predictions are consistent with observations of flume studies (Finnegan et al., 2007).

Results from previous work that include sediment dynamics has suggested lower sensitivity of river steepness in response to rock uplift than what is predicted by the 1-D detachment-limited models (Cowie et al., 2008; DiBiase et al., 2010; Ouimet et al., 2009; Whittaker et al., 2007a). Suggestions for the lower sensitivity have ranged from the effects of sediment (Cowie et al., 2008; Gasparini et al., 2007) to variability in water discharge (DiBiase & Whipple, 2011; Scherler et al., 2017). Although I did not specifically explore discharge variability, I expect it would act to further lower the sensitivity between rock uplift and steepness as found in previous work. Further work will explore the relative impacts of sediment discharge, water discharge, and channel width changes in determining how these different factors each contribute to influencing channel response to rock uplift. Nonetheless, when considering the observations of transient river morphology (both slope and width) and steady state systems (quantifying the relationship between steepness and rock uplift), the combined impacts of sediment dynamics and channel width changes are likely to be an important factor in controlling topographic response to tectonics in many river systems.

In summary, 1-D approaches that do not account for channel width adjustments and models that ignore the impacts of sediment likely overestimate the topographic response to a change in rock uplift. Observations of channel width adjustment and channels laden with sediment are common in natural settings, suggesting that the effects modeled here are likely important in many tectonic and climatic settings around the world. This has implications for modeling the coupling of climate-tectonics and the prediction of topographic response to dynamic mantle processes (Braun et al., 2013; Roe & Brandon, 2011; Whipple & Meade, 2006; Willett, 1999).

5.2. Thoughts on Field Observations

5.2.1. Observations of Width in Transient Systems

An observation in many natural systems is that during the passage of a transient wave of incision, the river systems tends to narrow (Ouimet et al., 2008; Reusser et al., 2004; Valla et al., 2010). In many locations, the channel then widens following the passage of the transient signal or knickzone (Amos & Burbank, 2007; Finnegan et al., 2007; Kirby & Ouimet, 2011; Whitbread et al., 2015; Whittaker et al., 2007a; Yanites et al., 2018). The modeling results presented here suggest that this behavior is a symptom of sediment transport dynamics playing a key role in controlling the channel morphology of these actively eroding river systems. This interpretation is based on the consistency of the field observations with the predictions of the sediment cover and saltation-abrasion models presented here but not the pure bedrock detachment-limited model. In the detachment-limited runs (both BR-DL and SC-DL), the system narrows in response to the steepening and increase in erosion rate (e.g., Finnegan et al., 2005; Wobus, Tucker, & Anderson 2006). The narrow width persists after the transient wave has passed in the BR-DL model but not in any of the sediment dependent models. In the sediment-dependent runs, the system can narrow during the transience and behaves similarly to the detachment limited model runs such as in the SC-DL and SA-TL runs. This is due to the relatively high base level fall and low sediment supply. But as the transient wave migrates upstream, the increase in sediment load drives widening and further steepening of the downstream reaches (e.g., Figures 6 and 9). The modeling approach presented here can capture the shift in limitations of bedrock erosion (e.g., detachment versus exposure limited) that can occur during a transient response. For example, during transience of exposure-limited systems (e.g., SC-EL), the systems effectively become detachment-limited but then return to exposure limited following the passage of the knickzone. Other field-based evidence consistent with the interpretation that sediment supply influences channel width is the observation of channel narrowing following dam construction (Richard et al., 2005) which is a recent perturbation that lowers sediment supply.

5.2.2. Erosional Controls Reflected in Channel Morphology?

The different morphological responses to a change in rock uplift in rivers suggest that observations of both width and the 1-D river profile (e.g., slope and concavity) can provide important insights into the underlying mechanisms controlling river dynamics. The addition of observations of width, along with patterns of channel slope, can help decipher if a system transitions from exposure- to detachment-limited behavior during transience. This provides an extra level of observation beyond relying only on the channel profile during transients to decipher the underlying control on erosion in actively incising river systems (Tucker & Whipple,

2002; Whipple & Tucker, 2002). For example, channel widening downstream of a knickzone that is generated due to an increase in rock uplift can only be reproduced in sediment-dependent models. The biggest signal of widening due to increased sediment supply occurs when the system is swamped with sediment (i.e., F is very low) and becomes bedrock exposure-limited. Conversely, detachment-limited behavior will result in channel narrowing that remains narrow following the passage of the knickzone. Such predictions could be consistent with the maintenance of a deep, narrow gorge following the passage of a knickzone (Whipple, Snyder, et al., 2000). Conditions for both detachment- and exposure-limited controls on river incision likely exist in natural settings; however, observations of the channel profile alone are unlikely to reveal differences in these erosional mechanisms, especially if the system transitions from exposure-limited to detachment-limited during transience. Based on the results of this modeling exercise, I suggest that with careful examination of both the profile and channel width through a transient system, one can gain more insight into the mechanisms controlling river dynamics (Whittaker et al., 2007a).

5.3. Consideration of Climatic Impacts

Although the model runs here focus on tectonic changes in rock uplift, some discussion on how changes in climate could influence the systems is warranted. In the detachment-limited model, the prediction of climate change is clear in that any changes in precipitation will result in a corresponding change in the slope of the river, modulated by the concurrent change in width since the river is carrying a different discharge. The prediction is clear in that an increase in precipitation will lead to higher erosion potential, as the increase in discharge will outcompete the increase in channel width, which acts to lower shear stress. This will lower slopes and overall topographic relief.

How the sediment-dependent systems respond to a change in climate, however, is not as clear-cut. An increase in water discharge will increase sediment transport capacity and act to lower elevations. However, an increase in precipitation may also increase sediment supply, which, if the system is in an exposure-limited state, may act toward increasing elevations as less exposure will lower the erosional efficiency. Understanding the river response in these systems requires a more careful consideration of how changes in precipitation influence hillslope processes and sediment supply than I consider here. Nonetheless, this thought experiment brings up an important question that should be considered in future studies: Can an increase in precipitation enhance sediment supply from hillslopes resulting in greater fluvial relief? For this to occur, the increase in sediment supply must outweigh any increase in sediment transport capacity (equation (7)). Such a scenario would result in channel steepening, widening, and a short-term reduction in river incision rates, a potentially observable prediction. An alternative scenario in which sediment supply relative to transport capacity is reduced, perhaps due to aridification, could lead to channel narrowing (due to a reduction in sediment supply) and a pulse of incision into the landscape (e.g., Cooper et al., 2016; Malatesta et al., 2017). A pulse of incision in this scenario could be attributed to an increase in bedrock exposure. This occurrence might be indicative of the development of steep gorges inset into broad valleys in regions that have undergone a recent reduction in sediment supply such as in many deglaciated valleys. In any case, it is clear that when hillslope-channel coupling is important, considerations of how climate impacts orogen relief requires more careful consideration of how the entire landscape (hillslopes and rivers) are impacted by changes in precipitation. Because of this channel-hillslope coupling, a drainage basin with a bedrock exposure-limited river system is likely to experience hillslope erosion and channel incision that are out of phase with one another as climate fluctuates.

6. Conclusions

I have presented a new approach to modeling river systems that erode bedrock. The model can account for dynamic channel width and the effects of sediment transport. The results presented here are consistent with previous work that suggests caution is needed when making interpretations based only on the 1-D stream power model, though there are likely natural settings in which proper calibration of the model will capture the relevant physics of river dynamics. In general, the results of this study show that incorporating channel width into a detachment-limited model makes the river profile less sensitive to changes in rock uplift than the 1-D approach. This is because changes in channel width accommodate some of the geomorphic response to a change in rock uplift. When sediment transport dynamics are considered, the sensitivity to rock uplift is further reduced. How much of a change occurs, however, depends on the degree to which the

system is exposure-limited versus detachment- or tools-limited. The state of the system is controlled by the relative importance of sediment supply, sediment caliber, bedrock erosional resistance, and the rock-uplift rate, which also ultimately controls sediment supply. For example, a landscape with relatively weak rock that has a high supply of bedload sediment (e.g., due to high rock-uplift rates) will tend toward the exposure-limited spectrum of bedrock river dynamics, whereas a system with low sediment supply (perhaps due to low rock uplift), but less erosive rocks, will tend toward the detachment/tools limited endmember. In the exposure-limited cases, the channels counterintuitively widen in response to an increase in rock uplift. This is because of the strong influence of sediment supply on width in these environments. An advantage of the modeling approach developed here is that further insight into the physical factors controlling incision can be gained by observing channel width and slope during the transient response of a river system to a change in external forcing. Finally, incorporating both channel width adjustments and sediment transport dynamics into models of river response has important implications for modeling the interactions among climate, tectonics, and landscape evolution.

Acknowledgments
The author was supported by National Science Foundation EAR-1251377 and Indiana University's Center for Pervasive Technology. Research was sponsored by the Army Research Laboratory and was accomplished under grant W911NF-17-1-0248. The views and conclusions contained in this document are those of the authors and should not be interpreted as representing the official policies, either expressed or implied, of the Army Research Laboratory or the U.S. Government. The U.S. Government is authorized to reproduce and distribute reprints for Government purposes notwithstanding any copyright notation herein. This manuscript benefited from thorough reviews and comments by Aaron Bufe, Burch Fisher, an anonymous reviewer, Associate Editor Mikael Attal, and Editor John Buffington. The model codes are hosted on the CSDMS model repository (https://csdms.colorado.edu/wiki/Model:OTTER), and model results are stored on Indiana University's Scholarly Data Archive (http://hdl.handle.net/2022/21949).

References

Allen, G. H., Barnes, J. B., Pavelsky, T. M., & Kirby, E. (2013). Lithologic and tectonic controls on bedrock channel form at the northwest Himalayan front. *Journal of Geophysical Research: Earth Surface*, *118*, 1806–1825. https://doi.org/10.1002/jgrf.20113

Amos, C. B., & Burbank, D. W. (2007). Channel width response to differential uplift. *Journal of Geophysical Research*, *112*, F02010. https://doi.org/10.1029/2006JF000672

Attal, M., & Lavé, J. (2006). Changes of bedload characteristics along the Marsyandi River (Central Nepal): Implications for understanding hillslope sediment supply, sediment load evolution along fluvial networks, and denudation in active orogenic belts. *Geological Society of America Special Papers*, *398*, 143–171. https://doi.org/10.1130/2006.2398(09)

Attal, M., Tucker, G. E., Whittaker, A. C., Cowie, P. A., & Roberts, G. P. (2008). Modeling fluvial incision and transient landscape evolution: Influence of dynamic channel adjustment. *Journal of Geophysical Research*, *113*, F03013. https://doi.org/10.1029/2007JF000893

Barnhart, C. J., Howard, A. D., & Moore, J. M. (2009). Long-term precipitation and late-stage valley network formation: Landform simulations of Parana Basin, Mars. *Journal of Geophysical Research*, *114*, E01003. https://doi.org/10.1029/2008JE003122

Braun, J., Robert, X., & Simon-Labric, T. (2013). Eroding dynamic topography. *Geophysical Research Letters*, *40*, 1494–1499. https://doi.org/10.1002/grl.50310

Brocard, G. Y., & van der Van Der Beek, P. A. (2006). Influence of incision rate, rock strength, and bedload supply on bedrock river gradients and valley-flat widths: Field-based evidence and calibrations from western Alpine rivers (Southeast France). *Geological Society of America Special Papers*, *398*, 101–126. https://doi.org/10.1130/2006.2398(07)

Brocard, G. Y., Willenbring, J. K., Miller, T. E., & Scatena, F. N. (2016). Relict landscape resistance to dissection by upstream migrating knickpoints. *Journal of Geophysical Research: Earth Surface*, *121*, 1182–1203. https://doi.org/10.1002/2015JF003678

Bufe, A., Paola, C., & Burbank, D. W. (2016). Fluvial bevelling of topography controlled by lateral channel mobility and uplift rate. *Nature Geoscience*, *9*(9), 706–710. https://doi.org/10.1038/ngeo2773

Bull, W. B. (1990). Stream-terrace genesis: Implications for soil development. *Geomorphology*, *3*(3-4), 351–367. https://doi.org/10.1016/0169-555X(90)90011-E

Chen, C.-Y., & Willett, S. D. (2016). Graphical methods of river profile analysis to unravel drainage area change, uplift and erodibility contrasts in the central range of Taiwan. *Earth Surface Processes and Landforms*, *41*(15), 2223–2238. https://doi.org/10.1002/esp.3986

Coleman, T., & Li, Y. (1996). An interior trust region approach for nonlinear minimization subject to bounds. *SIAM Journal on Optimization*, *6*(2), 418–445. https://doi.org/10.1137/0806023

Cooper, F. J., Adams, B. A., Blundy, J. D., Farley, K. A., McKeon, R. E., & Ruggiero, A. (2016). Aridity-induced Miocene canyon incision in the Central Andes. *Geology*, *44*(8), 675–678. https://doi.org/10.1130/G38254.1

Cowie, P. A., Whittaker, A. C., Attal, M., Roberts, G., Tucker, G. E., & Ganas, A. (2008). New constraints on sediment-flux–dependent river incision: Implications for extracting tectonic signals from river profiles. *Geology*, *36*(7), 535–538. https://doi.org/10.1130/G24681A.1

Crosby, B. T., & Whipple, K. X. (2006). Knickpoint initiation and distribution within fluvial networks: 236 waterfalls in the Waipaoa River, North Island, New Zealand. *Geomorphology*, *82*(1–2), 16–38. https://doi.org/10.1016/j.geomorph.2005.08.023

Crosby, B. T., Whipple, K. X., Gasparini, N. M., & Wobus, C. W. (2007). Formation of fluvial hanging valleys: Theory and simulation. *Journal of Geophysical Research*, *112*, F03S10. https://doi.org/10.1029/2006JF000566

Cyr, A. J., Granger, D. E., Olivetti, V., & Molin, P. (2010). Quantifying rock uplift rates using channel steepness and cosmogenic nuclide-determined erosion rates: Examples from northern and southern Italy. *Lithosphere*, *2*(3), 188–198. https://doi.org/10.1130/L96.1

DiBiase, R. A., & Whipple, K. X. (2011). The influence of erosion thresholds and runoff variability on the relationships among topography, climate, and erosion rate. *Journal of Geophysical Research*, *116*, F04036. https://doi.org/10.1029/2011JF002095

DiBiase, R. A., Whipple, K. X., Heimsath, A. M., & Ouimet, W. B. (2010). Landscape form and millennial erosion rates in the San Gabriel Mountains, CA. *Earth and Planetary Science Letters*, *289*(1–2), 134–144. https://doi.org/10.1016/j.epsl.2009.10.036

Duvall, A., Kirby, E., & Burbank, D. (2004). Tectonic and lithologic controls on bedrock channel profiles and processes in coastal California. *Journal of Geophysical Research*, *109*, F03002. https://doi.org/10.1029/2003JF000086

Exner, F. M. (1920). Zur physik der dünen, Hölder.

Exner, F. M. (1925). Uber die wechselwirkung zwischen wasser und geschiebe in flussen, Akad. der Wiss in Wien, Math-Naturwissenschafliche Klasse, Sitzungsberichte. *Abt IIa*, *134*, 165–203.

Ferrier, K. L., Huppert, K. L., & Perron, J. T. (2013). Climatic control of bedrock river incision. *Nature*, *496*(7444), 206–209. https://doi.org/10.1038/nature11982

Finnegan, N. J., & Dietrich, W. E. (2011). Episodic bedrock strath terrace formation due to meander migration and cutoff. *Geology*, *39*(2), 143–146. https://doi.org/10.1130/G31716.1

Finnegan, N. J., Roe, G., Montgomery, D. R., & Hallet, B. (2005). Controls on the channel width of rivers: Implications for modeling fluvial incision of bedrock. *Geology*, *33*(3), 229–232. https://doi.org/10.1130/G21171.1

Finnegan, N. J., Sklar, L. S., & Fuller, T. K. (2007). Interplay of sediment supply, river incision, and channel morphology revealed by the transient evolution of an experimental bedrock channel. *Journal of Geophysical Research*, *112*, F03S11. https://doi.org/10.1029/2006JF000569

Flint, J. J. (1974). Stream gradient as a function of order, magnitude, and discharge. *Water Resources Research*, *10*, 969–973. https://doi.org/10.1029/WR010i005p00969

Forte, A. M., Yanites, B. J., & Whipple, K. X. (2016). Complexities of landscape evolution during incision through layered stratigraphy with contrasts in rock strength. *Earth Surface Processes and Landforms*, *41*(12), 1736–1757. https://doi.org/10.1002/esp.3947

Gasparini, N. M., & Whipple, K. X. (2014). Diagnosing climatic and tectonic controls on topography: Eastern flank of the northern Bolivian Andes. *Lithosphere*, *6*(4), 230–250. https://doi.org/10.1130/L322.1

Gasparini, N. M., Whipple, K. X., & Bras, R. L. (2007). Predictions of steady state and transient landscape morphology using sediment-flux-dependent river incision models. *Journal of Geophysical Research*, *112*, F03S09. https://doi.org/10.1029/2006JF000567

Goren, L., Fox, M., & Willett, S. D. (2014). Tectonics from fluvial topography using formal linear inversion: Theory and applications to the Inyo Mountains, California. *Journal of Geophysical Research: Earth Surface*, *119*, 1651–1681. https://doi.org/10.1002/2014JF003079

Hack, J. T. (1957). *Studies of longitudinal stream profiles in Virginia and Maryland*. Washington, DC: U.S. Government Printing Office.

Hancock, G. S., & Anderson, R. S. (2002). Numerical modeling of fluvial strath-terrace formation in response to oscillating climate. *Geological Society of America Bulletin*, *114*(9), 1131–1142. https://doi.org/10.1130/0016-7606(2002)114<1131:NMOFST>2.0.CO;2

Hancock, G. S., Small, E. E., & Wobus, C. (2011). Modeling the effects of weathering on bedrock-floored channel geometry. *Journal of Geophysical Research*, *116*, F03018. https://doi.org/10.1029/2010JF001908

Howard, A. D. (1994). A detachment-limited model of drainage basin evolution. *Water Resources Research*, *30*(7), 2261–2285. https://doi.org/10.1029/94WR00757

Howard, A. D., & Kerby, G. (1983). Channel changes in badlands. *Geological Society of America Bulletin*, *94*(6), 739–752. https://doi.org/10.1130/0016-7606(1983)94<739:CCIB>2.0.CO;2

Jansen, J. D., Fabel, D., Bishop, P., Xu, S., Schnabel, C., & Codilean, A. T. (2011). Does decreasing paraglacial sediment supply slow knickpoint retreat? *Geology*, *39*(6), 543–546. https://doi.org/10.1130/G32018.1

Jeffery, M. L., Ehlers, T. A., Yanites, B. J., & Poulsen, C. J. (2013). Quantifying the role of paleoclimate and Andean Plateau uplift on river incision. *Journal of Geophysical Research: Earth Surface*, *118*, 852–871. https://doi.org/10.1002/jgrf.20055

Johnson, J. P. L., Whipple, K. X., Sklar, L. S., & Hanks, T. C. (2009). Transport slopes, sediment cover, and bedrock channel incision in the Henry Mountains, Utah. *Journal of Geophysical Research*, *114*, F02014. https://doi.org/10.1029/2007JF000862

Kirby, E., & Ouimet, W. (2011). Tectonic geomorphology along the eastern margin of Tibet: Insights into the pattern and processes of active deformation adjacent to the Sichuan Basin. *Geological Society, London, Special Publications*, *353*(1), 165–188. https://doi.org/10.1144/SP353.9

Kirby, E., & Whipple, K. (2001). Quantifying differential rock-uplift rates via stream profile analysis. *Geology*, *29*(5), 415–418. https://doi.org/10.1130/0091-7613(2001)029<0415:QDRURV>2.0.CO;2

Kirby, E., & Whipple, K. X. (2012). Expression of active tectonics in erosional landscapes. *Journal of Structural Geology*, *44*, 54–75. https://doi.org/10.1016/j.jsg.2012.07.009

Kooi, H., & Beaumont, C. (1994). Escarpment evolution on high-elevation rifted margins: Insights derived from a surface processes model that combines diffusion, advection, and reaction. *Journal of Geophysical Research*, *99*, 12,191–12,209. https://doi.org/10.1029/94JB00047

Lague, D. (2010). Reduction of long-term bedrock incision efficiency by short-term alluvial cover intermittency. *Journal of Geophysical Research*, *115*, F02011. https://doi.org/10.1029/2008JF001210

Lague, D. (2014). The stream power river incision model: Evidence, theory and beyond. *Earth Surface Processes and Landforms*, *39*(1), 38–61. https://doi.org/10.1002/esp.3462

Langston, A. L., & Tucker, G. E. (2018). Developing and exploring a theory for the lateral erosion of bedrock channels for use in landscape evolution models. *Earth Surface Dynamics*, *6*(1), 1–27. https://doi.org/10.5194/esurf-6-1-2018

Lavé, J., & Avouac, J. P. (2001). Fluvial incision and tectonic uplift across the Himalayas of Central Nepal. *Journal of Geophysical Research*, *106*, 26,561–26,591. https://doi.org/10.1029/2001JB000359

Limaye, A. B. S., & Lamb, M. P. (2016). Numerical model predictions of autogenic fluvial terraces and comparison to climate change expectations. *Journal of Geophysical Research: Earth Surface*, *121*, 512–544. https://doi.org/10.1002/2014JF003392

Malatesta, L. C., Avouac, J. P., Brown, N. D., Breitenbach, S. F. M., Pan, J., Chevalier, M. L., et al. (2017). Lag and mixing during sediment transfer across the Tian Shan piedmont caused by climate-driven aggradation-incision cycles. *Basin Research*. https://doi.org/10.1111/bre.12267

Meyer-Peter, E., & Müller, R. (1948). Formulas for bed-load transport, IAHR.

Montgomery, D. R., & Gran, K. B. (2001). Downstream variations in the width of bedrock channels. *Water Resources Research*, *37*, 1841–1846. https://doi.org/10.1029/2000WR900393

Murphy, B. P., Johnson, J. P. L., Gasparini, N. M., & Sklar, L. S. (2016). Chemical weathering as a mechanism for the climatic control of bedrock river incision. *Nature*, *532*(7598), 223–227. https://doi.org/10.1038/nature17449

Nanson, G. C., & Huang, H. Q. (2008). Least action principle, equilibrium states, iterative adjustment and the stability of alluvial channels. *Earth Surface Processes and Landforms*, *33*(6), 923–942. https://doi.org/10.1002/esp.1584

Nelson, P. A., & Seminara, G. (2011). Modeling the evolution of bedrock channel shape with erosion from saltating bed load. *Geophysical Research Letters*, *38*, L17406. https://doi.org/10.1029/2011GL048628

Ouimet, W. B., Whipple, K. X., Crosby, B. T., Johnson, J. P., & Schildgen, T. F. (2008). Epigenetic gorges in fluvial landscapes. *Earth Surface Processes and Landforms*, *33*(13), 1993–2009. https://doi.org/10.1002/esp.1650

Ouimet, W. B., Whipple, K. X., & Granger, D. E. (2009). Beyond threshold hillslopes: Channel adjustment to base-level fall in tectonically active mountain ranges. *Geology*, *37*(7), 579–582. https://doi.org/10.1130/G30013A.1

Paola, C., & Voller, V. R. (2005). A generalized Exner equation for sediment mass balance. *Journal of Geophysical Research*, *110*, F04014. https://doi.org/10.1029/2004JF000274

Pazzaglia, F. J., Gardner, T. W., & Merritts, D. J. (1998). Bedrock fluvial incision and longitudinal profile development over geologic time scales determined by fluvial terraces. *Geophysical Monograph-American Geophysical Union*, *107*, 207–236.

Pelletier, J. D. (2007). Numerical modeling of the Cenozoic geomorphic evolution of the southern Sierra Nevada, California. *Earth and Planetary Science Letters*, *259*(1–2), 85–96. https://doi.org/10.1016/j.epsl.2007.04.030

Perne, M., Covington, M. D., Thaler, E. A., & Myre, J. M. (2017). Steady state, erosional continuity, and the topography of landscapes developed in layered rocks. *Earth Surface Dynamics*, *5*(1), 85–100. https://doi.org/10.5194/esurf-5-85-2017

Perron, J. T., & Royden, L. (2013). An integral approach to bedrock river profile analysis. *Earth Surface Processes and Landforms*, *38*(6), 570–576. https://doi.org/10.1002/esp.3302

Reusser, L. J., Bierman, P. R., Pavich, M. J., Zen, E.-A., Larsen, J., & Finkel, R. (2004). Rapid late Pleistocene incision of Atlantic passive-margin river gorges. *Science*, *305*(5683), 499–502. https://doi.org/10.1126/science.1097780

Richard, G. A., Julien, P. Y., & Baird, D. C. (2005). Case study: Modeling the lateral mobility of the Rio Grande below Cochiti Dam, New Mexico. *Journal of Hydraulic Engineering*, *131*(11), 931–941. https://doi.org/10.1061/(ASCE)0733-9429(2005)131:11(931)

Roberts, G. G., & White, N. (2010). Estimating uplift rate histories from river profiles using African examples. *Journal of Geophysical Research*, *115*, B02406. https://doi.org/10.1029/2009JB006692

Roe, G. H., & Brandon, M. T. (2011). Critical form and feedbacks in mountain-belt dynamics: Role of rheology as a tectonic governor. *Journal of Geophysical Research*, *116*, B02101. https://doi.org/10.1029/2009JB006571

Roe, G. H., Montgomery, D. R., & Hallet, B. (2002). Effects of orographic precipitation variations on the concavity of steady-state river profiles. *Geology*, *30*(2), 143. https://doi.org/10.1130/0091-7613(2002)030<0143:EOOPVO>2.0.CO;2

Royden, L., & Perron, J. T. (2013). Solutions of the stream power equation and application to the evolution of river longitudinal profiles. *Journal of Geophysical Research: Earth Surface*, *118*, 497–518. https://doi.org/10.1002/jgrf.20031

Scherler, D., DiBiase, R. A., Fisher, G. B., & Avouac, J.-P. (2017). Testing monsoonal controls on bedrock river incision in the Himalaya and Eastern Tibet with a stochastic-threshold stream power model. *Journal of Geophysical Research: Earth Surface*, *122*, 1389–1429. https://doi.org/10.1002/2016JF004011

Seeber, L., & Gornitz, V. (1983). River profiles along the Himalayan arc as indicators of active tectonics. *Tectonophysics*, *92*(4), 335–367. https://doi.org/10.1016/0040-1951(83)90201-9

Sklar, L. S., & Dietrich, W. E. (2004). A mechanistic model for river incision into bedrock by saltating bed load. *Water Resources Research*, *40*, W06301. https://doi.org/10.1029/2003WR002496

Sklar, L. S., & Dietrich, W. E. (2006). The role of sediment in controlling steady-state bedrock channel slope: Implications of the saltation-abrasion incision model. *Geomorphology*, *82*(1–2), 58–83. https://doi.org/10.1016/j.geomorph.2005.08.019

Snyder, N. P., Whipple, K. X., Tucker, G. E., & Merritts, D. J. (2000). Landscape response to tectonic forcing: Digital elevation model analysis of stream profiles in the Mendocino triple junction region, northern California. *Geological Society of America Bulletin*, *112*(8), 1250–1263. https://doi.org/10.1130/0016-7606(2000)112<1250:LRTTFD>2.0.CO;2

Snyder, N. P., Whipple, K. X., Tucker, G. E., & Merritts, D. J. (2003). Importance of a stochastic distribution of floods and erosion thresholds in the bedrock river incision problem. *Journal of Geophysical Research*, *108*(B2), 2117. https://doi.org/10.1029/2001JB001655

Stark, C. P. (2006). A self-regulating model of bedrock river channel geometry. *Geophysical Research Letters*, *33*, L04402. https://doi.org/10.1029/2005GL023193

Sternberg, H. (1875). Untersuchungen u¨ber La¨ngen-und Querprofil geschiebefu¨hrender Flu¨sse, Zeitschrift fu¨r. *Bauwesen*, *25*, 483–506.

Tucker, G. E. (2004). Drainage basin sensitivity to tectonic and climatic forcing: Implications of a stochastic model for the role of entrainment and erosion thresholds. *Earth Surface Processes and Landforms*, *29*(2), 185–205. https://doi.org/10.1002/esp.1020

Tucker, G. E., & Whipple, K. X. (2002). Topographic outcomes predicted by stream erosion models: Sensitivity analysis and intermodel comparison. *Journal of Geophysical Research*, *107*(B9), 2179. https://doi.org/10.1029/2001JB000162

Turowski, J. M., & Hodge, R. (2017). A probabilistic framework for the cover effect in bedrock erosion. *Earth Surface Dynamics*, *5*(2), 311–330. https://doi.org/10.5194/esurf-5-311-2017

Turowski, J. M., Lague, D., & Hovius, N. (2007). Cover effect in bedrock abrasion: A new derivation and its implications for the modeling of bedrock channel morphology. *Journal of Geophysical Research*, *112*, F04006. https://doi.org/10.1029/2006JF000697

Turowski, J. M., Lague, D., & Hovius, N. (2009). Response of bedrock channel width to tectonic forcing: Insights from a numerical model, theoretical considerations, and comparison with field data. *Journal of Geophysical Research*, *114*, F03016. https://doi.org/10.1029/2008JF001133

Turowski, J. M., Rickenmann, D., & Dadson, S. J. (2010). The partitioning of the total sediment load of a river into suspended load and bedload: A review of empirical data. *Sedimentology*, *57*(4), 1126–1146. https://doi.org/10.1111/j.1365-3091.2009.01140.x

Valla, P. G., Van Der Beek, P. A., & Carcaillet, J. (2010). Dating bedrock gorge incision in the French Western Alps (Ecrins-Pelvoux massif) using cosmogenic 10Be. *Terra Nova*, *22*(1), 18–25. https://doi.org/10.1111/j.1365-3121.2009.00911.x

Ward, D. J., & Galewsky, J. (2014). Exploring landscape sensitivity to the Pacific Trade Wind Inversion on the subsiding island of Hawaii. *Journal of Geophysical Research: Earth Surface*, *119*, 2048–2069. https://doi.org/10.1002/2014JF003155

Whipple, K. X. (2001). Fluvial landscape response time: How plausible is steady-state denudation? *American Journal of Science*, *301*(4–5), 313–325. https://doi.org/10.2475/ajs.301.4-5.313

Whipple, K. X., Hancock, G. S., & Anderson, R. S. (2000). River incision into bedrock: Mechanics and relative efficacy of plucking, abrasion, and cavitation. *Geological Society of America Bulletin*, *112*(3), 490–503. https://doi.org/10.1130/0016-7606(2000)112<490:RIIBMA>2.0.CO;2

Whipple, K. X., & Meade, B. J. (2006). Orogen response to changes in climatic and tectonic forcing. *Earth and Planetary Science Letters*, *243*(1–2), 218–228. https://doi.org/10.1016/j.epsl.2005.12.022

Whipple, K. X., Snyder, N. P., & Dollenmayer, K. (2000). Rates and processes of bedrock incision by the Upper Ukak River since the 1912 Novarupta ash flow in the Valley of Ten Thousand Smokes, Alaska. *Geology*, *28*(9), 835–838. https://doi.org/10.1130/0091-7613(2000)28<835:RAPOBI>2.0.CO;2

Whipple, K. X., & Tucker, G. E. (1999). Dynamics of the stream-power river incision model: Implications for height limits of mountain ranges, landscape response timescales, and research needs. *Journal of Geophysical Research*, *104*, 17,661–17,674. https://doi.org/10.1029/1999JB900120

Whipple, K. X., & Tucker, G. E. (2002). Implications of sediment-flux-dependent river incision models for landscape evolution. *Journal of Geophysical Research*, *107*(B2), 2039. https://doi.org/10.1029/2000JB000044

Whitbread, K., Jansen, J., Bishop, P., & Attal, M. (2015). Substrate, sediment, and slope controls on bedrock channel geometry in postglacial streams. *Journal of Geophysical Research: Earth Surface*, *120*, 779–798. https://doi.org/10.1002/2014JF003295

Whittaker, A. C., Cowie, P. A., Attal, M., Tucker, G. E., & Roberts, G. P. (2007a). Bedrock channel adjustment to tectonic forcing: Implications for predicting river incision rates. *Geology*, *35*(2), 103–106. https://doi.org/10.1130/G23106A.1

Whittaker, A. C., Cowie, P. A., Attal, M., Tucker, G. E., & Roberts, G. P. (2007b). Contrasting transient and steady-state rivers crossing active normal faults: New field observations from the Central Apennines, Italy. *Basin Research*, *19*(4), 529–556. https://doi.org/10.1111/j.1365-2117.2007.00337.x

Willett, S. D. (1999). Orogeny and orography: The effects of erosion on the structure of mountain belts. *Journal of Geophysical Research*, *104*, 28,957–28,981. https://doi.org/10.1029/1999JB900248

Wobus, C., Whipple, K. X., Kirby, E., Snyder, N., Johnson, J., Spyropolou, K., et al. (2006). Tectonics from topography: Procedures, promise, and pitfalls. *Geological Society of America Special Papers*, *398*, 55–74. https://doi.org/10.1130/2006.2398(04)

Wobus, C. W., Tucker, G. E., & Anderson, R. S. (2006). Self-formed bedrock channels. *Geophysical Research Letters*, *33*, L18408. https://doi.org/10.1029/2006GL027182

Wobus, C. W., Tucker, G. E., & Anderson, R. S. (2010). Does climate change create distinctive patterns of landscape incision? *Journal of Geophysical Research*, *115*, F04008. https://doi.org/10.1029/2009JF001562

Wong, M., & Parker, G. (2006). Reanalysis and correction of bed-load relation of Meyer-Peter and Müller using their own database. *Journal of Hydraulic Engineering*, *132*(11), 1159. https://doi.org/10.1061/(ASCE)0733-9429(2006)132:11

Yanites, B. J., Ehlers, T. A., Becker, J. K., Schnellmann, M., & Heuberger, S. (2013). High magnitude and rapid incision from river capture: Rhine River, Switzerland. *Journal of Geophysical Research: Earth Surface*, *118*, 1060–1084. https://doi.org/10.1002/jgrf.20056

Yanites, B. J., Mitchell, N. A., Bregy, J. C., Carlson, G. A., Cataldo, K., Holahan, M., et al. (2018). Landslides control the spatial and temporal variation of channel width in southern Taiwan: Implications for landscape evolution and cascading hazards in steep, tectonically active landscapes. *Earth Surface Processes and Landforms*. https://doi.org/10.1002/esp.4353

Yanites, B. J., & Tucker, G. E. (2010). Controls and limits on bedrock channel geometry. *Journal of Geophysical Research*, *115*, F04019. https://doi.org/10.1029/2009JF001601

Yanites, B. J., Tucker, G. E., Hsu, H.-L., Chen, C., Chen, Y.-G., & Mueller, K. J. (2011). The influence of sediment cover variability on long-term river incision rates: An example from the Peikang River, central Taiwan. *Journal of Geophysical Research*, *116*, F03016. https://doi.org/10.1029/2010JF001933

Yanites, B. J., Tucker, G. E., Mueller, K. J., Chen, Y.-G., Wilcox, T., Huang, S.-Y., & Shi, K.-W. (2010). Incision and channel morphology across active structures along the Peikang River, Central Taiwan: Implications for the importance of channel width. *Geological Society of America Bulletin*, *122*(7–8), 1192–1208. https://doi.org/10.1130/B30035.1

Zhang, H., Kirby, E., Pitlick, J., Anderson, R. S., & Zhang, P. (2017). Characterizing the transient geomorphic response to base-level fall in the northeastern Tibetan Plateau. *Journal of Geophysical Research: Earth Surface*, *122*, 546–572. https://doi.org/10.1002/2015JF003715